WHERE THE ZIGZAGS GO: A MICROHABITAT ANALYSIS FOR THE *PLETHODON DORSALIS* COMPLEX WITHIN THE TENNESSEE RIVER GORGE

By

Tegan Childers

Thomas P. Wilson
UC Foundation Professor of
Biology, Geology, and Environmental Science
(Chair)

A.K.M. Azad Hossain
Assistant Professor of Biology,
Geology, and Environmental Science
(Committee Member)

Sumith Gunasekera
Associate Professor, Mathematics
(Committee Member)

Bradley R. Reynolds
Senior Lecturer of Biology,
Geology, and Environmental Science
(Committee Member)

WHERE THE ZIGZAGS GO: A MICROHABITAT ANALYSIS FOR THE *PLETHODON DORSALIS* COMPLEX WITHIN THE TENNESSEE RIVER GORGE

By

Tegan Childers

A Thesis Submitted to the Faculty of the University of
Tennessee at Chattanooga in Partial
Fulfillment of the Requirements of the Degree
of Master of Science: Environmental Science

The University of Tennessee at Chattanooga
Chattanooga, Tennessee

June 2020

ABSTRACT

Northern Zigzag salamanders (*Plethodon dorsalis*) are an understudied bioindicator of many ecosystems in the southeastern United States. Population sampling is conducted within the Tennessee River Gorge by surveying three 2,000 m² sites from October 28, 2018 to June 8, 2019. Landscape data are mapped using ArcGIS. Salamanders are located using a time-based natural cover object survey method. Microhabitat is analyzed within 1 m² of each location using paired locations for presence and absence. This assessment attempts to identify differences in microhabitat preference based on selected versus available habitat using predictive geospatial models and AICc values. These AICc values demonstrate the performance of covariates measured and model fit in relation to salamander presence. Results support that different factors influence the distribution of *P. dorsalis* with respect to microhabitat selection, and conservation and management recommendations are discussed.

DEDICATION

This work is dedicated to my grandmother Elsie Kirk, my parents Jane and Dean Hendricks, and my husband Christian Childers. You know what you did.

ACKNOWLEDGEMENTS

I would like to start by thanking my committee members Dr. Hossain, Dr. Gunasekera, and Dr. Reynolds for their patience, support, and guidance. Their input has been critical to my success in developing my thesis.

Many Team Salamander members, friends and peers were kind enough to take time out of their lives to support my work as well. John Shelton assisted with ground-truthing to confirm land cover types. Rick Blanton provided assistance with spatial data acquisition. Field survey volunteers included Michael Ashcraft, Rachel Head, Garrett Holder, Jarid Prahl, Katie Quast, Bianca Bradshaw, Sarah Kelehear, Kelly Daniels, Paul-Erik Bakland, Tanner Gatlin, Cassandra Gilmore, Cullen Harris, Nate Parrish and Erin Taylor. Breanna McDevitt deserves special mention as the most consistent and most patient member of my field survey team. She has endured the bulk of challenging field conditions met during this work. Tucker Clark and Yatri Patel wrote, modified, and explicated a Python script to help me transform my data for analysis.

Daley Harrison was my first ever research partner during my undergraduate work. Her partnership gave me the confidence to peruse challenges I never would have tried to face alone.

Nyssa Hunt has provided assistance in nearly every aspect of this project. Her guidance and unwavering patience is a primary reason for my skill development with GIS and overall morale. Nyssa has consistently been a fantastic friend, lab mate and teacher.

Chris Manis and John Lugthart are the reasons I even considered applying to graduate school. Their dedication as my undergraduate research advisors and mentors has been incredibly

valuable. They provided me with the opportunities I needed to develop my own intrinsic value in the research sciences.

Dr. Wilson, as my graduate advisor and mentor, has guided me through the most challenging years of my life. I will never be able to thank him enough for his time and dedication. Without him, I would never have gotten this far. He truly taught me what it means to be a great scientist.

TABLE OF CONTENTS

LIST OF TABLES

LIST OF FIGURES

LIST OF ABBREVIATIONS

AIC, Akaike Information Criterion

AICc, Corrected Akaike Information Criterion

DEM, Digital Elevation Model

GAP, Gap Analysis Program

GIS, Geographic Information Systems

GPS, Global Positioning System

GWR, Geographic Weighted Regression

LIDAR, Light Detection and Ranging

NLCD, National Land Cover Database

NAIP, National Agriculture Imagery Program

OLS, Ordinary Least Squares

SAS, Statistical Analysis Software

SPSS, Statistical Package for the Social Sciences

TDEC, Tennessee Department of Environment and Conservation

TRG, Tennessee River Gorge

USDA, United States Department of Agriculture

USGS, United States Geological Survey

CHAPTER I

THE PLACE OF *PLETHODON DORSALIS* WITHIN THE LANDSCAPE OF THE TENNESSEE RIVER GORGE

Introduction

Relevance of Amphibian Conservation

As earth's biodiversity faces tremendous loss, it is apparent that amphibian taxa are fielding the greater proportion of this loss among other vertebrate groups (Baillie, 2004; Blaustein, Walls & Bancroft et al., 2010; Shinwari, Gilani & Kahn, 2012). Knowing that these sensitive creatures serve as bioindicators for the overall health and quality of many ecosystems (Shinwari, Gilani, & Kahn, 2012), we should aim to comprehend their habitat requirements. Establishing these data could ultimately allow conservationists to set accurate baselines for various mitigation and land management practices (Shoo, Olson & McMenamin, 2011). Here I look specifically to the Northern Zigzag salamander (*Plethodon dorsalis*) because much like its closely related sister taxa, it too may be a high biomass species (Burton, 1975; Jaeger, 1979; Dillard, Russell & Ford, 2008), and at this time, there is a lack of fine scale habitat data for this species in the literature (Britton, 1981).

Spatial Distribution of Plethodon dorsalis

Occurring through most of Kentucky, reaching upwards through all of southern and much of central Indiana, this salamander's range covers a large swath of the eastern United States (Petranka, 1998; Baillie, 2004; Powell, Conant & Collins, 2016). There are also records of *P. dorsalis* through south and east Illinois (Petranka, 1998; Baillie, 2004; Powell, Conant & Collins, 2016). Tennessee's range of *P. dorsalis* has not been officially discerned from that of its physically identical sister taxa, *P. ventralis* (Niemiller & Reynolds, 2011). It is suspected that *P. dorsalis* ranges across most of central and east Tennessee (Petranka, 1998; Baillie, 2004; Powell, Conant & Collins, 2016). In this study, I focus on *P. dorsalis* populations within the Tennessee River Gorge (TRG).

Description of the Tennessee River Gorge

Enveloping the Tennessee River, the TRG is a 41 km long section comprised of a 10,926 ha expanse of river canyon (Blyveis, 2011; Youngman, 2017). Upon the Cumberland Plateau it reaches from west of Chattanooga at William's Island to Nickajack Dam just south of Jasper, TN, and is overlooked by Walden's Ridge to the north and Aetna Mountain to the south (Blyveis, 2011; Youngman, 2017). Characterized primarily by oak-hickory stands, the TRG also contains variations in understory cover and soil types (Blyveis, 2011; Youngman, 2017). Approximately 75% of the land within the TRG is collectively protected by either the Tennessee Wildlife Resources Agency, the Tennessee Valley Authority, the Tennessee River Gorge Trust, or private owners via conservation easements (Youngman, 2017).

Relevance of Land Cover Assessment

It is known that no segment of an ecosystem functions entirely independent of any other segment, be it biotic or abiotic; all parts are affected by one another. Land cover types often have broad and varied influences on understory and micro story structure that can accommodate or exclude life, including amphibians (Dupuis, Smith & Bunnell, 1995; Compton, Rhymer & McCollough, 2002; Dillard, Russell & Ford, 2008; Shinwari, Gilani & Kahn, 2012). Knowing land cover types and their distribution provides guiding information for habitat analysis on both large and small-scale projects (Weih & Riggan, 2010; Rozenstein & Karnieli, 2011). By beginning the site selection process with a geospatial, meso scale analysis of land cover types in the TRG, I can minimize the risk of large-scale differences in habitats skewing the data at the microhabitat scale.

Research Questions

The primary research objectives investigated in this study are:

1. Can *P. dorsalis* be located across multiple elevations in the TRG?
2. What land cover types are present across the elevation gradient in the TRG?
3. Can land cover data help identify proportionate representations of land cover types across an elevation gradient in the TRG?

Methods

Plethodon dorsalis Presence

To begin identifying potential survey areas, I collected occurrence data on *P. dorsalis* from three sources, Vert Net, iNaturalist and United States Geological Survey (USGS), all of which were similar to current range maps (Powell, Conant & Collins, 2016). Species occurrence data were accessed through the Vert Net open data portal, a National Science Foundation funded website. Research grade location data was acquired through iNaturalist, a citizen science website. Some data points included records near the intended survey area of the TRG. Species range data from the USGS Gap Analysis Program (GAP) were applied, and represent a coarse scale of suspected range for *P. dorsalis*. Range data from USGS for *P. dorsalis* and *P. ventralis* suggested that their range overlaps, and *P. ventralis* may be the species being addressed in this study. Data sets for *P. dorsalis* were uploaded into ArcGIS Pro and input onto a base map for simultaneous review as seen in Figure 1. On an outing in October of 2017, Team Salamander (Team Salamander is the herpetology lab founded and operated by Dr. Thomas P. Wilson at the University of Tennessee at Chattanooga) confirmed the presence of *P. dorsalis* along the Lower Pot Point Trail numerous times across the elevation gradient.

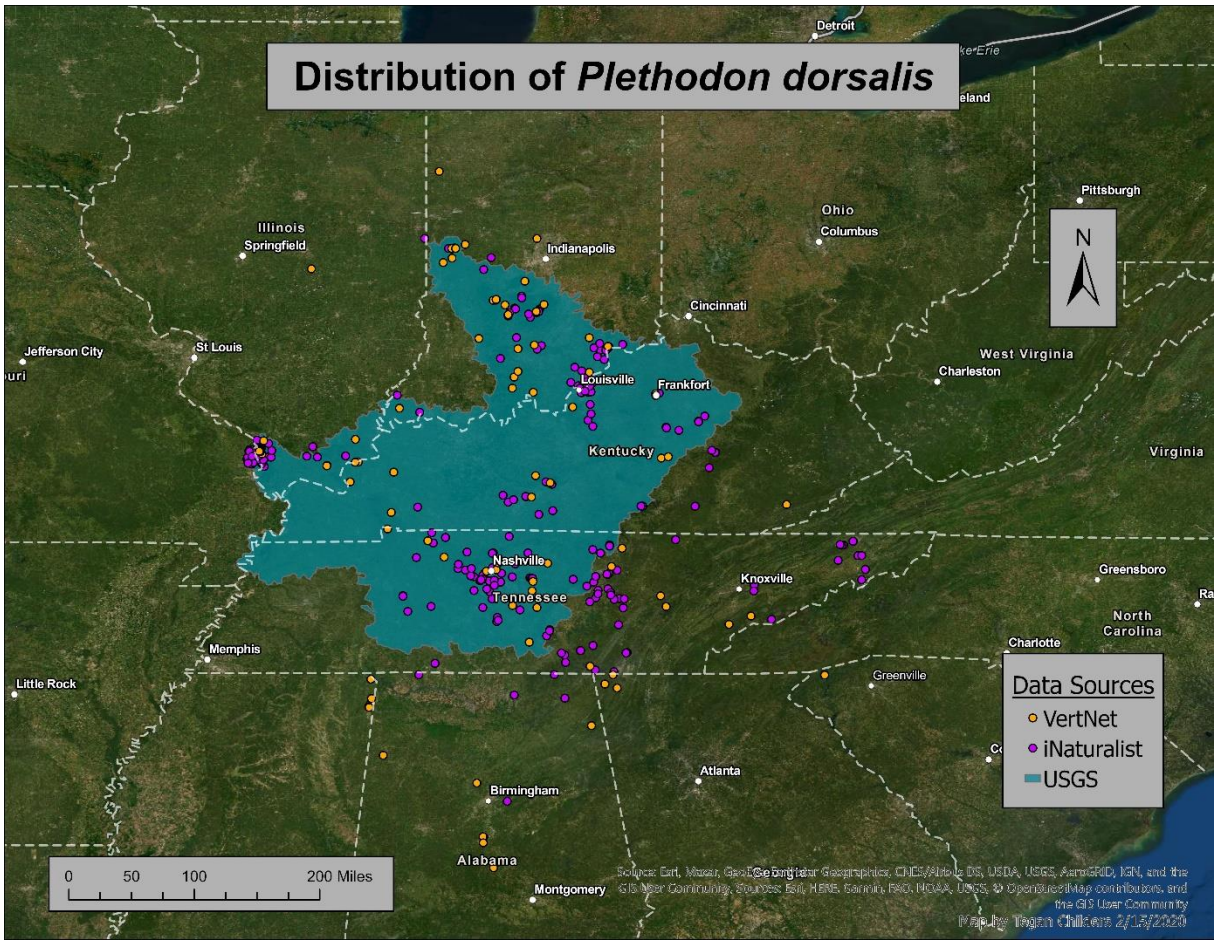

Figure 1 A collective representation of *P. dorsalis* locations and suspected range (Datum: NAD_1983_ North American 1983)

Selection and Acquisition of Land Cover Data Sources

ArcMap 10.6 was used to evaluate three separate land cover data sources within a 200 m buffer of the Lower Pot Point Trail. Buffer size was selected to encompass multiple elevations; this way trends could be assessed across the elevation gradient. Thirty meter resolution data was sourced from USGS in the form of National Land Cover Database (NLCD) from 2011 and TN GAP data from 2011. One-meter resolution data was sourced from the National Agriculture Imagery Program (NAIP) generated by the United States Department of Agriculture (USDA) in 2017. This range of data set resolutions provided both a meso and micro scale component to the assessment. An additional 3 m light detection and ranging (LIDAR) based digital elevation model (DEM) was acquired from the USDA to view divisions along the elevation gradient, and refine survey location planning.

Analysis of Data Sources

Tennessee state plane projection was chosen for land cover because it was designed to minimize map distortion specifically for the state of Tennessee, and therefore was deemed most suitable for research working with land cover data specific to the state. Data for the NLCD and TN GAP land cover classes were reviewed and compared visually. Image classification was applied to the NAIP data through both supervised and unsupervised classification because land cover classes were not yet assigned to the imagery (Weih & Riggan, 2010; Rozenstein & Karnieli, 2011). Extract by mask was applied to the original data sets; this tool essentially removed extraneous areas of data so that supervised classifications would be more efficient. Unsupervised classification did not support the use of extract by mask. Supervised classification

utilized the maximum likelihood classification tool, which used training samples of the different class types based on their associated colors. Training samples were built by choosing multiple representative pixels for each land cover class. Each set of samples were identified by the tool and the selected pixels were merged into their respective representative samples for the different land cover classes. An interactive supervised classification function was applied using information from the training samples. Iso-cluster unsupervised classification was processed with all three data sets for comparison. The iso-cluster option reclassified with minimal user input, and because of this, was less prone to user error. Combining the functionalities of the iso-cluster and maximum likelihood classification tools, the isodata clustering algorithm determined the number of characteristics within the natural groupings of cells.

Accuracy Assessments for Land Cover Classifications

To confirm proportional representation of land cover types, an in situ ground-truthing assessment was performed. Ground-truthing was applied to ensure that the satellite data provided an accurate representation of land cover composition for all imagery sources. For this process, ten random points were generated within the 200 m trail buffer and assessed for land cover representation. Types of trees were recorded within approximately ten meters of each random point. After reviewing the assessments, survey polygons were generated in ArcMap 10.6 and then reviewed on the ground to avoid selection bias. Areas with unmanageably steep terrain or overwhelmingly thick understory were excluded from survey consideration when encountered. Final survey polygon designations at the 250-300, 300-350 and 350-400 m elevations were identified as Elevation 1 (e1), Elevation 2 (e2) and Elevation 3 (e3).

Selection of Survey Polygon Locations

Survey polygon locations were determined based on their distance from roads or trails, distribution across elevations, proportional representation of land cover, and ability to be traversed. To prevent additional human interference, survey polygons were located a minimum of 50 m from roads or trails. Each polygon had to be in separate 50 m elevation windows, and over 90 m apart from each other. Such a large separation of survey polygons allows for differences across the elevation gradient to be assessed, and it would be unlikely that salamanders were crossing in between the different survey polygons (Kleeberger & Werner, 1982). For better representation of land cover types, the aforementioned accuracy assessments were used to target areas of the forest that proportionately represented the majority of land cover within the 200 m^2 trail buffer.

Results

Confirmation of Plethodon dorsalis Presence

Target species are successfully located across the 250-300, 300-350 and 350-400 m elevations on exploratory searches in both the fall of 2017 and the spring of 2018. During these preliminary searches, salamanders are present under various natural cover objects primarily comprising of rocks, logs and leaf litter. Preliminary search methods at each elevation window include random searching along an approximate 50 m buffer of the trail, searching pre-planned 100 m tangents and searching connected tangents of 25 m that randomly change angle at the end of each tangent. UX Apps provides the random angles for the connected tangents. My final and

highest yielding search method proves to be searching a pre-planned survey polygon. Using this method, I walked across the entirety of the polygon while searching under all natural cover objects that I came across. Final polygon designations are determined in situ confirmation of salamanders a thorough review of land cover composition, additional in situ confirmation of salamander presence and in situ confirmation for the ability to traverse the area without damaging the habitat.

Composition of Land Cover Types

Preprocessed NLCD data for the state of Tennessee has 20 classes, and only five of those represent land cover within a 200 m buffer of the Lower Pot Point Trail. These habitat classes include open water, barren rock, mixed forest, deciduous forest, and herbaceous wetland (Figure 2.1). Tennessee GAP data are set in 77 representative classes; six of these are within the 200 m buffer of the trail. These habitat classes include open water, open rock and boreal cliff, temperate flooded swamp forest and floodplain, Appalachian central mesic interior forest, southern oak-hickory-pine forest and oak-hardwood-pine dry calcareous forest (Figure 2.2). Ortho rectified imagery is from the NAIP data, and therefore it has no assigned classes. Despite manually identifying multiple different spectral signatures through training samples, the supervised classification aggregates all classes within the buffer into a single class (Figure 2.3). An unsupervised classification provides five different classes; one was clearly associated with open water, and another with cloud cover or barren rock (Figure 2.4). The other three classes are intermingled across the majority of the forest as a large mosaic. In situ ground-truthing confirms

trends in land cover distribution and identifies multiple areas as potentially suitable for survey assessments.

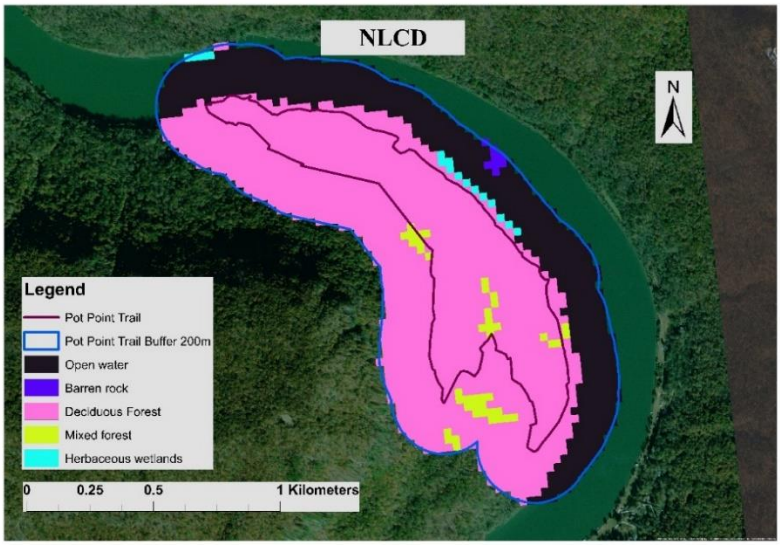

Figure 2.1 NLCD data for the 200 m buffer around the Pot Point Trail (Datum: NAD_1983_2011, Coordinate system: StatePlane_ Tennessee_FIPS_4100_Ft_US)

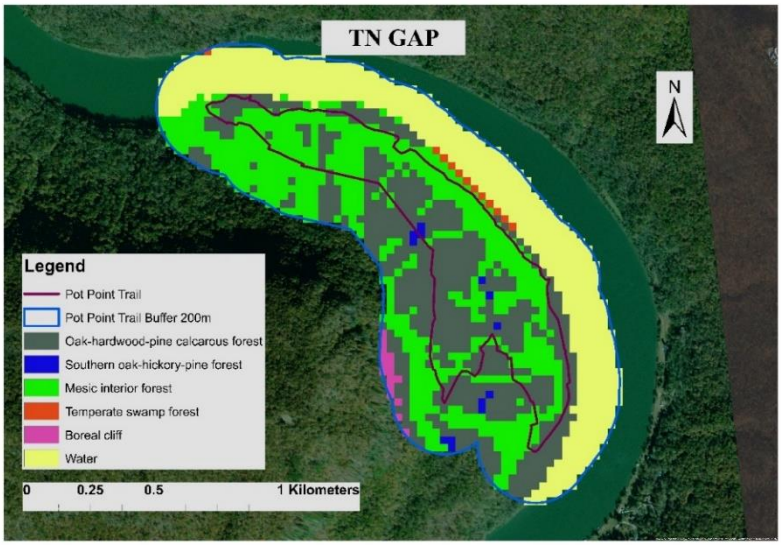

Figure 2.2 TN GAP data for the 200 m buffer around the Pot Point Trail (Datum: NAD_1983_2011, Coordinate system: StatePlane_ Tennessee_FIPS_4100_Ft_US)

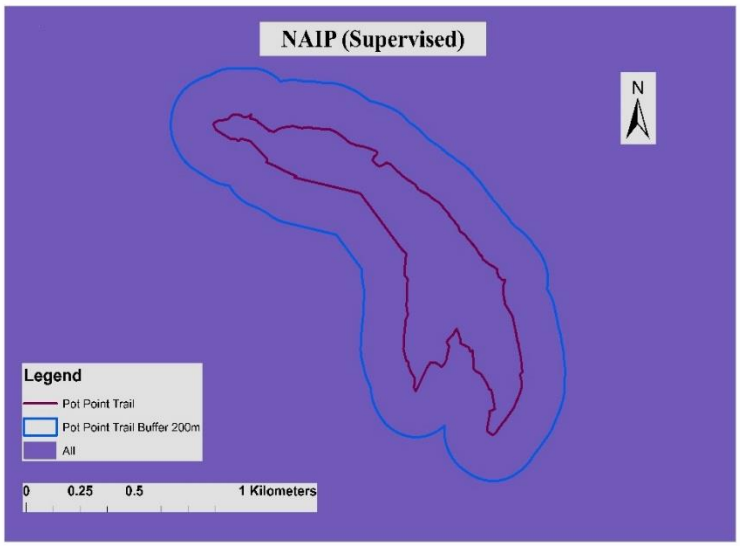

Figure 2.3 Supervised classification of NAIP data for the 200 m buffer around the Pot Point Trail (Datum: NAD_1983_2011, Coordinate system: StatePlane_ Tennessee_FIPS_4100_Ft_US)

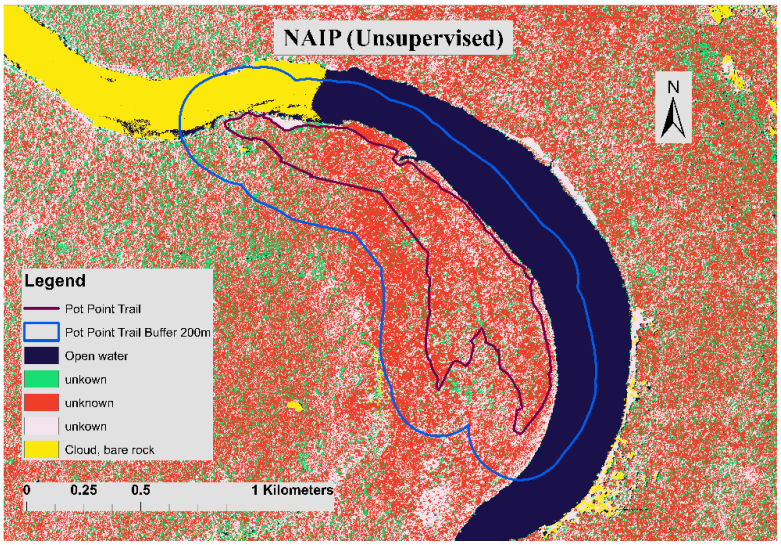

Figure 2.4 Unsupervised classification of NAIP data for the 200 m buffer around the Pot Point Trail (Datum: NAD_1983_2011, Coordinate system: StatePlane_ Tennessee_FIPS_4100_Ft_US)

Distribution of Survey Polygons

Survey polygons cover three elevations at the 250-300, 300-350 and 350-400 m range. It is not feasible to survey at a lower elevation because this places survey polygons too close to the road, trails or the river. Surveying is also restricted from higher elevations because the topography shifts from gradual slopes into steep cliffs. Overwhelmingly thick understory growth, that is too thick to navigate without destroying the habitat, rules out a potential location at the 350-400 m range. Unmanageably steep terrain with loose soil prevents the use of a potential location at the 300-350 m range. There are also multiple dead trees across the stretch that fall down the slope when disturbed. I have also disqualified an initially sampled e1 candidate at the 250-300 m range. This location has virtually no salamander presence when compared to the same or other elevations from early summer to late fall of 2018. More large boulders and rocks are present at this location than all other areas considered.

Locations that meet the criteria for survey polygons are each approximately 2000 m^2 (Figure 3). The final polygon designations at the 250-300, 300-350 and 350-400 m elevations are Elevation 1 (e1), Elevation 2 (e2) and Elevation 3 (e3). Though these polygons covered areas that proportionally represent the land cover classed across the 200 m buffer, the understory and micro story flora are visually unique.

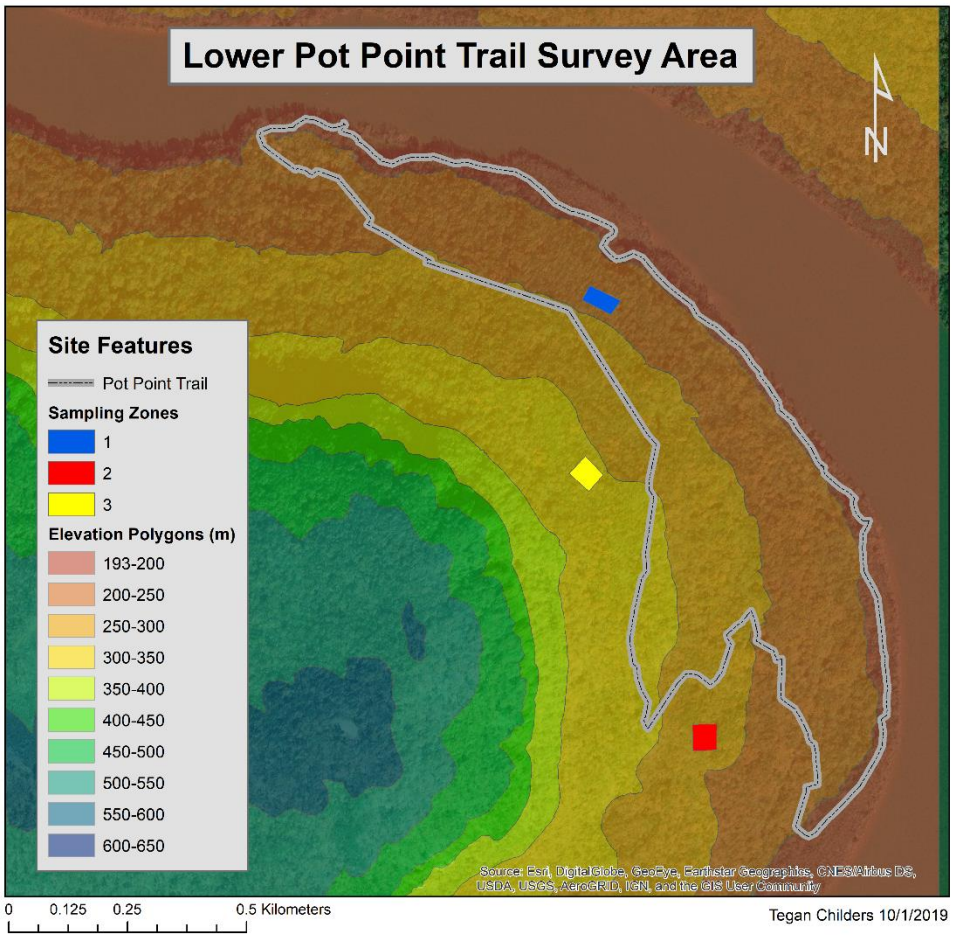

Figure 3 Distribution of three survey polygons around the Pot Point Trail (Datum: NAD_1983_2011, Coordinate system: StatePlane_ Tennessee_FIPS_4100_Ft_US)

Discussion

Finding Plethodon dorsalis

Officially, I began my field season in September but after a very dry summer the *P. dorsalis* did not emerge above the soil until October 28th, 2018. Three to four times a month, throughout the early fall; I search across the slopes of the Lower Pot Point Trail but have few to no sightings of *P. dorsalis*. During this period, the only terrestrial salamanders present above the soil were Northern slimy salamander (*Plethodon glutinosus*). After nearly two months of continuous searching within my pre-assigned survey polygons, and sporadically along the trails, *P. dorsalis* emerge from the soil along with the occurrence of back-to-back heavy cool rains. Once fall weather is cool and damp, these salamanders are abundant in e2 and e3 survey polygons. A stark lack of salamanders in the original e1 polygon initiates a search to establish a new e1 polygon as previously discussed in this chapter's methods and results.

Land Cover Qualities

Imagery from the NLCD data, from my interpretation, oversimplifies the diversity of the forest within the sampling buffer. This imagery also interprets a space in the middle of the river to be a rock. When looking out over the river, no rocks are visible at this location, and it is not apparent on other maps. I suspect that the barren rock class is due to reflectance from watercraft, low water levels, or mixed pixel effects. Tennessee GAP imagery represents Oak-hardwood-pine dry calcareous forest as the majority of land cover within the buffer. Appalachian central mesic interior forest is the second most prevalent and southern oak-hickory-pine forest is the third.

Moisture retention qualities between these two forest types are similar when contrasted against the Oak-hardwood-pine dry calcareous forest. Combined, these three classes represent the majority of space within the designated buffer. Unsupervised NAIP data appears to be the best representation for the pattern of broad diversity within a predominantly oak-hickory forest. Interpreting the unsupervised NAIP information in conjunction with the more specifically refined classes in the supervised TN GAP data seems ideal because it helps to paint a more detailed picture with its structural designations. Ground-truthing best supported the representation provided by NAIP data as a spectral mosaic under the unsupervised analysis. Based on the accuracy assessments and ground-truthing efforts, data class configurations from the USGS and USDA appear to be generally consistent with the forest composition.

Survey Polygon Locations

My initial e1 sample site is far more densely populated with large rocks and boulders, but seemingly unpopulated by salamanders when compared to the other sample sites throughout the summer and during the first few weeks of *P. dorsalis* emergence in the fall. Such loose, rocky habitat composition is more difficult to search without altering the habitat. It is possible that I have a bias in my thinking that this particular area has a low density of salamanders. I cannot say if the initial e1 location truly has fewer salamanders present or if it is just harder to search effectively due to the habitat structure. It is possible that this area appears to have fewer salamanders because the terrain is more difficult to search without altering the habitat. This issue drove me to examine another space in the lower elevation window that also meets the aforementioned boundaries. Salamanders are more easily located at the second e1 location

considered, and is now e1 for continued sampling. If it is necessary to search this type of habitat structure in the future, I suggest investing in a probe style camera designed for crevices.

The site first considered for e2 is sparsely vegetated, with loose soil, and multiple dead trees that easily fell if disturbed. This site promptly excludes surveying because of an apparent lack of salamanders, and an excess of unmanageable terrain. Notably, the final e2 survey polygon has a thicker understory than the other elevations and it is primarily comprised of young beech trees. On the first day of sampling, salamanders are easily located under natural cover objects. At the highest surveyed elevations, e3 has the highest occurrence of salamanders on the first day of sampling. This is unsurprising because the e3 survey polygon is about 200 m away from a steep and rocky cliff face. Literature shows that *P. dorsalis* and its sister taxa are sometimes present in similar habitats.

Conclusion

Through a mixture of the application of species occurrence data and land cover imagery, survey polygons for e1, e2 and e3 are established. These areas identified as e1, e2 and e3 all have salamander presence and are viable for researching the microhabitat preference of *P. dorsalis*. Land cover assessments leading to these designated survey polygons are most effective when simultaneously applied. Accuracy assessments provide better perspective on the qualities of overall land cover composition. Though they were generally similar, no individual data set generated a completely accurate picture of what ground truthing efforts reflect.

Largely, these methods can apply to simplifying the process of identifying valuable study areas for *P. dorsalis* and potentially other terrestrial salamanders. Planning study areas by

utilizing species occurrence data and remotely sensed information saves immense amounts of time, energy and resources.

CHAPTER II

STATISTICAL AND SPATIAL ANALYSIS OF *PLETHODON DORSALIS* MICROHABITAT PREFERENCE

Introduction

Variation within the Genus Plethodon

There is ecologic, and phenotypic variation in the family Plethodontidae, but some species of the Plethodon group may appear ecologically or physically similar even though they are genetically or geographically distinct (Highton, 1997; Highton, 1999; Petranka, 1998). Physical similarities among Plethodontidae include, but are not limited to, pigmentation, dorsal pattern, body length, and overall body mass (Highton, 1997; Highton, 1999; Petranka, 1998). A level of ecological equivalence is demonstrated in the comparison of *P.* dorsalis, and its sister taxa the Southern zigzag salamander (*P. ventralis*), the Southern red backed salamander (*P. serratus*), the Ozark zigzag salamander (*P. d. angusticlavius*), and the Red backed salamander (*P. cinereus*) (Highton, 1997; Petranka, 1998).

Variation within the Plethodon dorsalis Complex

As genetic analysis has become more accessible, researchers have described three species that were once all considered to be *P. dorsalis*. Thurow (1956) first determines that populations of suspected *P. dorsalis* are actually *P.d. angusticlavius*; this discovery confirms a genetic division in his effort to define salamander species rages (Thurow, 1957). Larson and Highton (1978) documents significantly distinct differences in the genetics of populations once assumed to be *P. dorsalis* in, and the species is later described as Webster's salamander (*Plethodon websteri*) (Highton, 1979). While assessing *P. dorsalis* species range, Highton (1997) establishes there is a 13 km hybridization zone of *P. dorsalis* and *P. ventralis*. The *P. dorsalis* species complex is cryptic in appearance and limited in ecological or behavioral differences, though it has significantly genetically distinct divisions. Due to minimal literature being available on the species of *P. dorsalis*, I apply information on some of its sister taxa to support the following study.

Home Range Retention and Territoriality

An example of genetically distinct sister taxa, the *P. serratus* has a known range that is adjacent to that of *P. dorsalis* along the borders of Northwestern Georgia, and Southeastern Tennessee (Petranka, 1998; Powell, Conant & Collins, 2016). This species exhibits, like many other salamanders, pheromone marking as a way of laying claim to its territory (Mathis, Deckard & Duer, 1998). In a lab setting, researchers document that pheromone marking in *P. serratus* provides a boundary observed by other salamanders (Mathis, Deckard & Duer, 1998). When

boundaries are crossed *P. serratus* takes aggressive action to remove intruders (Mathis, Deckard & Duer, 1998; Schieltz, Haywood & Marsh, 2010).

Plethodontids such as *P.d. angusticlavius* do not move far from their burrow, cave or general breeding site (Briggler & Puckette, 2003). Brooding females may use a single cave for at least a two-year period (Briggler & Puckette, 2003). Another study found that *P. cinereus* can maintain a home range for up to 151 days (Kleeberger & Werner, 1982). The largest mean home range record is for females with a mean activity radius of 24.34 ± 7.81 m (Kleeberger & Werner, 1982). When displaced 30 m from its home the salamander will make it back to its original home range at a rate of 80%, and when displaced 90 m the salamanders return at a rate of 25% (Kleeberger et al. 1982). Within those returns, half of the salamanders are found at the exact site they are displaced from while the other half are found within what is recognized as that individuals home range (Kleeberger & Werner, 1982).

When removing *P. cinereus* from its defined home range it takes a total of 13 days ± 1 days to make it back to the original home range location across the maximum distance of 90 m (Kleeberger & Werner, 1982). Though the average daily movement in the active season is only 0.43 m per salamander (Kleeberger & Werner, 1982), it is clear that these small Plethodontids can have variation within their ranges of activity.

Considering a species retains (Briggler & Puckette, 2003; Kleeberger & Werner, 1982), marks (Mathis, Deckard & Duer, 1998) and defends (Highton, 1999; Mathis, Deckard & Duer, 1998; Schieltz, Haywood & Marsh, 2010) a home range, it seems reasonable to investigate if the salamanders select their home ranges randomly. I address here if a sample population of terrestrial Plethodontids, primarily *P. dorsalis*, in the TRG appear to choose their habitat randomly or with certain microhabitat attributes in mind. Comparing both continuous and

dichotomous data on microhabitat structure at individual elevations and across elevations sheds some light on this concept. The null hypothesis of this study it that *P. dorsalis* does not exhibit any habitat preference.

Microhabitat Suitability Modeling

Multi-criteria decision making models (MCDMs) are a form of suitability modeling and an established technique that applies to addressing multi-factor spatial problems (Carver, 1991; Bonissone, Subbu & Lizzi, 2009). Suitability models of this type provide the opportunity to look at each factor with both unweighted and various weighted perspectives. Meaning, all microhabitat covariates compare equally, or with different values of importance attached to each covariate. In this case, I am attempting to identify preferred habitat of *P. dorsalis*. By classifying, aggregating and weighting data on physical structures and macro scale effects, I aim to establish a data set of this species microhabitat covariate preference.

Research Questions

The primary research objectives investigated in this study are:

1. Do *P. dorsalis* exhibit microhabitat preference within and across elevations along the slopes of the Lower Pot Point Trail in the TRG?
2. Do predictive microhabitat models concur with field observations of *P. dorsalis*?

Methods

Specimen Location

Sampling of survey polygons began on October 28, 2018 when *P. dorsalis* was first seen above ground. The sampling concluded on June 8, 2019 when *P. dorsalis* could consistently no longer be located above ground. Pre-determined 2000 m² polygons at three elevations known as e1, e2 and e3 (250-300, 300-350 and 350-400 m) were surveyed no more than once a week in an attempt to less significantly influence the behavior of the salamanders (Marsh & Goicochea, 2003; Schieltz, Haywood & Marsh, 2010). These polygons, constructed with USGS 3 m resolution DEM data, represented similar land cover proportions seen across the 200 m trail buffer, as discussed in chapter one of this document. The polygons were separated by a minimum of 100 m because it has been documented that *P. cinereus* and other sister taxa to *P. dorsalis* will rarely move across such distance (Kleeberger & Werner, 1982; Smith & Green, 2005). Due to the lack of difference in size between *P. dorsalis* and its sister taxa (Highton, 1997; Petranka, 1998), it was predicted that these buffer zones would not be crossed. Natural cover surveys were conducted, so each potential natural cover object crossed was searched for salamanders when sweeping along the entirety of the 2000 m² polygon (Dodd, 2009). For consistency, search time while sweeping across the polygon was one hour; this did not account for data collection or any other time spent not actively looking for salamanders. For every terrestrial salamander located, a 1 m² grid was used to quantify animal presence covariates. In addition to this, a randomly chosen 1 m² grid absent of salamanders, within the survey polygon, was also located and documented for the same covariates. When a salamander was found, the salamander's location was mapped through the Mapit GIS application on an Android phone with

the assistance of a Trimble R-1 unit to amplify the accuracy of Global Positioning System (GPS) signal. A random number generator determined the angle and distance traveled within the polygon to locate the animal absence point. The randomly selected animal absence point was documented in the same fashion as the animal presence point.

Microhabitat Measurements

Data was collected by the quadrat using a 1 m^2 grid subdivided into 10 cm^2 increments. Quadrats were mapped, and measured for biophysical covariates at both the animal present and the paired, animal absent sites (Gustafson, Murphy & Crow, 2001; Compton, Rhymer & McCollough, 2002; Roe & Grayson, 2008; Groff, Calhoun & Loftin, 2016). A random number generator from UX Apps was used to determine the distance and angle for the location of each paired animal absence quadrat.

Each salamander present and absent quadrat was measured by analyzing a total of 23 covariates. These biophysical covariates were divided into three categories: weather and substrate temperatures, physical structures and macro scale effects. Weather and substrate temperatures included soil moisture, soil surface temperature, internal soil temperature, average wind speed, humidity, and air temperature. Physical structures included average leaf litter depth (cm), over story canopy estimated density, micro story canopy, leaf litter, moss cover, woody brush, coarse woody debris (diameter < 10 cm), logs (diameter > 10 cm), rocks (max diameter < 2 m) and boulders (max diameter > 2 m). Macro scale effects included land cover composition, elevation, slope and aspect.

Air temperature, humidity, and average wind speed were measured at the beginning of each survey session using a Kestrel weather meter. Soil surface temperature was taken using an Etekcity Lasergrip774 infrared thermometer, and internal soil temperature was measured with a five inch, stainless steel meat thermometer. Structure data was measured with either a ruler, or visually using the 10 cm^2 grid within the 1 m^2 grid tool. Macro scale effects data were derived from remotely sensed LIDAR data previously described in chapter one.

Site marking methods were implemented through a combination of multiple photos for identification, GPS points, and notes on landmarks. These measures allowed re-visitation of the quadrats while deterring locals from noticing markers used for the study. This was done with the intention to prevent additional outside and unnecessary sources of stress upon the salamanders being researched.

Statistical Analysis

Statistical analyses were applied for the composite of all three elevations and for each elevation individually. When assessing the raw data by testing for normality using the PROC UNIVARIATE statement with Statistical Analysis Software 9.4 (SAS) (see Appendix A), much of the data were non-parametric. All data in the physical structural category, and some weather and temperature data were non-parametric. Data were transformed using the Box Cox method in PyCharm (see appendix B). This transformation was applied to the non-parametric individual covariates. For example, all data on logs in a single elevation polygon were transformed as a set with their own best lambda value; this provided the most accurate transformation and prevents biased modeling.

Due to multicollinearity across all weather and temperature covariates, only soil surface temperature was included in the analysis. Over story canopy, average leaf litter depth and proportion of leaf litter coverage also show multicollinearity; of these three covariates, proportion of leaf litter coverage is used for this test. All other physical structures were included, excluding boulders because they were an outlier. Only one macro scale effect, slope, was considered due to multicollinearity with other macro scale effects.

A conditional logistic regression for matched pairs was applied using the PROC LOGISTIC statement in SAS (see Appendix A) to evaluate the animal presence and absence data (Compton, Rhymer & McCollough, 2002; Groff, Calhoun & Loftin, 2016). This test compared the dichotomous result of a salamander's absence or presence within the quadrats documented, while also comparing the continuous data and proportions measured within the same quadrats. Assumptions of this test include a linear relationship, multivariate normality, no or little multicollinearity, no auto-correlation and homoscedasticity. Additionally, there was a required sample size of at least 20 per independent variable in the analysis for this type of regression model.

The Akaike information criterion (Akaike, 1973) assessed the performance of covariates and model fit in relation to salamander presence (Mueller, Macey & Wake et al., 2004; Price, Eskew & Cecala, et al., 2012). The Wald Chi-Square value expressed model strength and significance. Wald Chi-Square values were also identified for the individual covariates to provide direct model value and significance.

Spatial Analysis

Spatial analyses were performed using animal presence data in ArcMap 10.6. Similar to the statistical analysis, proportion of leaf litter represents the over story canopy and average leaf litter depth covariates because of their multicollinearity. Boulders were once again excluded because they were an outlier. By reason of multicollinearity across all macro scale effects, slope was the only macro scale effect considered. Measurement data were input with their respective GPS points, summarized in Excel, and imported into ArcMap as a *.csv file. Display xy data plotted locations of the quadrat measurements as point data. Spline with barriers interpolated continuous surfaces for all structure covariates based on the quantities tied to the point data from the quadrats. On a scale of one to five, reclassify allowed for the development of a suitability ranking that provides classified interpretation of the data. Classes of five were the most highly associated with *P. dorsalis*, and classes of one were suspected to be the least suitable for the salamander. Classes were set by the frequency of salamanders associated with the proportional presence of each physical structure covariate. For example, if the majority of salamanders were found where five percent of the cover is moss, and no salamanders were found where the cover is zero percent moss, five percent moss might have a ranking of four or five where zero percent moss would have a ranking of zero. Once reclassify was applied, all surfaces were categorized with the same number of classes and the effects of multiple rasters were aggregated using raster calculator. Initially, this tool generated an unweighted multi criteria perspective where all values entered were equally represented. After that, a weighted version was processed where the total of all weights assigned would equal one. Listed in Table 1 are the assigned weights that are influenced by the values generated in the regression analysis. Weighting the model accounts for the differences in value of various microhabitat covariates.

Each suitability model was checked for accuracy using training samples in ArcPro. Subset features was applied to randomly isolate 80% of animal present points in separate survey polygons. I manually reviewed the training sample selection to assess the distribution of points in relation to the microhabitat suitability models.

Table 1 Weights applied to covariates for the weighted suitability models

Covariates	**e1**	**e2**	**e3**
microstory	0.2	0.2	0.05
leaflitter	0.025	0.2	0.1
moss	0.1	0.15	0.05
woody brush	0.1	0.05	0.2
coarse woody debris	0.1	0.15	0.2
logs	0.2	0.2	0.3
rocks	0.25	0.025	0.05
slope	0.025	0.025	0.05
Total weight =	1	1	1

Results

Statistical Analysis

All regression models are statistically significant with a *p*-value of < 0.05 or less as represented in Table 2; the majority of models have a higher level of significance. Table 2 details the list of results for the composite of all elevations and for each individual elevation. The top five models for each group are detailed in comparison to the original model. Levels of significance are as follows: * (≤ 0.01), ** (≤ 0.001), *** (≤ 0.0001), and all other *p*-values represent <0.05. The abbreviation for woody brush is wdybr, and the abbreviation for coarse woody debris is cwd. For the composite of all three elevations, the highest-ranking model is comprised of soil surface temperature, logs and rocks. At e1, the highest-ranking model is micro story, logs and rocks. Logs are the only variable in the highest-ranking model for e3, and the model for e2 consists of micro story and leaf litter.

Table 2 Conditional logistic regression for matched pairs results

		Covariates	AIC	AICc	Wald
All	**1**	soil surface temp, logs, rocks	375.244	375.381	37.2754***
All	**2**	logs, rocks	408.607	408.6834	32.0650***
All	**3**	soil surface temp, wdybr, logs, rocks	372.505	372.7116	40.2586***
All	**4**	soil surface temp, wdybr, cwd, logs, rocks	371.271	371.5614	42.2608***
All	**5**	soil surface temp, leaflitter, wdybr, cwd, logs, rocks	371.847	372.2357	42.8068***
All	**original**	soil surface temp, microstory, leaflitter, moss, wdybr, cwd, logs, rocks	372.289	372.9179	44.6480***
E1	**1**	microstory, logs, rocks	93.506	94.04696	16.0389**
E1	**2**	microstory, moss, logs, rocks	94.068	94.88949	16.3018*
E1	**3**	microstory, moss, wdybr, logs, rocks	94.638	95.80418	16.7915*
E1	**4**	microstory, moss, wdybr, cwd, logs, rocks	96.376	97.9538	16.6554*
E1	**5**	microstory, leaf litter, moss, wdybr, cwd, logs, rocks	97.556	99.61325	17.1638
E1	**original**	soil surface temp, microstory, leaflitter, moss, wdybr, cwd, logs, rocks	91.50237	94.35951	16.9025
E2	**1**	microstory, leaf litter	152.264	152.4779	11.2414*
E2	**2**	microstory, leaflitter, logs	151.103	151.4638	13.3698*
E2	**3**	microstory, leaflitter, cwd, logs	152.487	153.0328	13.6914*
E2	**4**	microstory, leaflitter, moss, logs	151.779	152.3246	14.1211*
E2	**5**	microstory, leaflitter, moss, cwd, logs	152.941	153.7118	14.7027*
E2	**original**	soil surface temp, microstory, leaflitter, moss, wdybr, cwd, logs, rocks	143.443	145.2984	17.5938
E3	**1**	logs	138.766	138.8657	26.9947***
E3	**2**	soil surface temp, logs	127.932	128.1477	27.0680***
E3	**3**	soil surface temp, wdybr, logs	126.92	127.2833	27.2815***
E3	**4**	soil surface temp, wdybr, cwd, logs	126.64	127.1907	27.9817***
E3	**5**	soil surface temp, leaflitter, wdybr, cwd, logs	127.394	128.1717	27.9532***
E3	**original**	soil surface temp, microstory, leaflitter, moss, wdybr, cwd, logs, rocks	133.351	135.0652	28.0483**

Spatial Analysis

Microhabitat suitability models are at a resolution of 2.5 m. Though the weather and physical structure data are collected at a 1 m^2 scale, the DEM from which macro scale effects are derived was at a 3 m resolution. While processing the point data into a continuous surface, the spline tool recommended this resolution. When compared against salamander presence and absence point data, the suitability models generally reflect the distribution of salamander presence across all three elevations (Figures 4.1, 4.2 and 4.3.). Exact pixel counts listed in Tables 3.1 and 3.2 detail the total distribution of ranks across the survey polygons. For unweighted models, the vast majority of pixels fall across the rank of three to four. In contrast to this, weighted model pixels primarily spread across the rank of four and five.

Spatial Accuracy Analysis

Tables 5 and 6 show the overall confirmation of suitability model accuracy when compared against the random subset of training samples. For all three elevations, the majority unweighted and weighted of training sample points fall in a suitability rank of three or higher. In the unweighted models for e1 and e2 there are zero points ranked as one, and in e3, only two points rank as one (Tables 4.1-4.3). Weighted models generated no data for the rank of one; consequently, no training point ranks as one (Tables 4.4-4.6). Even though weighted models generated data for the rank of two, no training points fall in the rank of two. Visual comparisons of animal presence point subsets with unweighted and weighted models are in Tables 4.7-4.12.

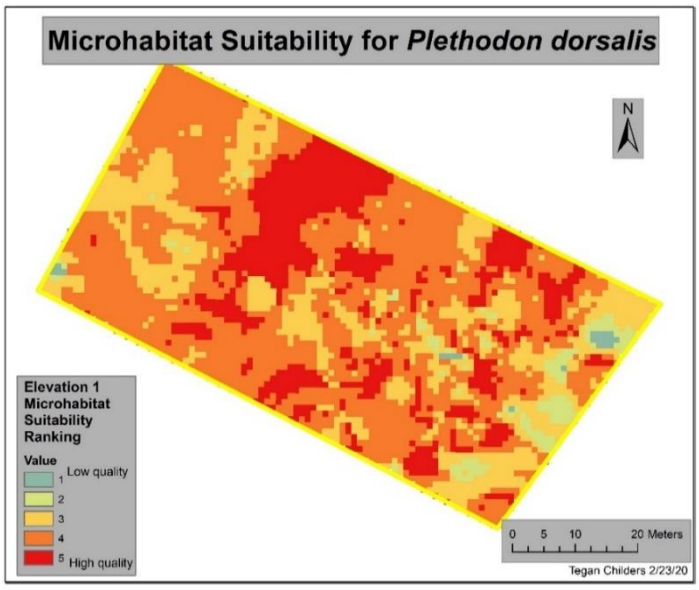

Figure 4.1 Microhabitat suitability model for e1 (Datum: NAD_1983_2011, Coordinate system: StatePlane_ Tennessee_FIPS_4100_Ft_US)

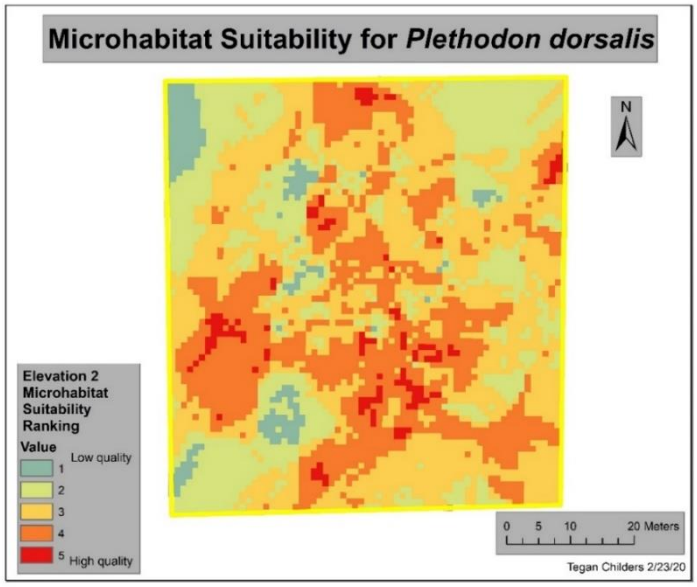

Figure 4.2 Microhabitat suitability model for e2 (Datum: NAD_1983_2011, Coordinate system: StatePlane_ Tennessee_FIPS_4100_Ft_US)

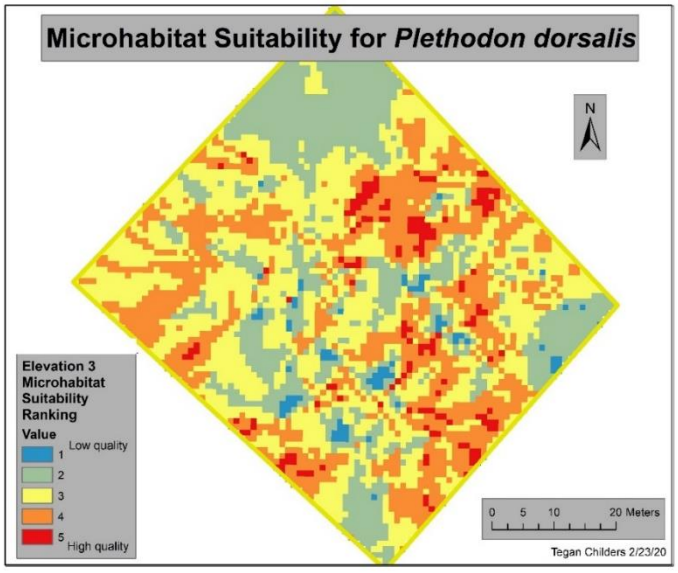

Figure 4.3 Microhabitat suitability model for e3 (Datum: NAD_1983_2011, Coordinate system: StatePlane_ Tennessee_FIPS_4100_Ft_US)

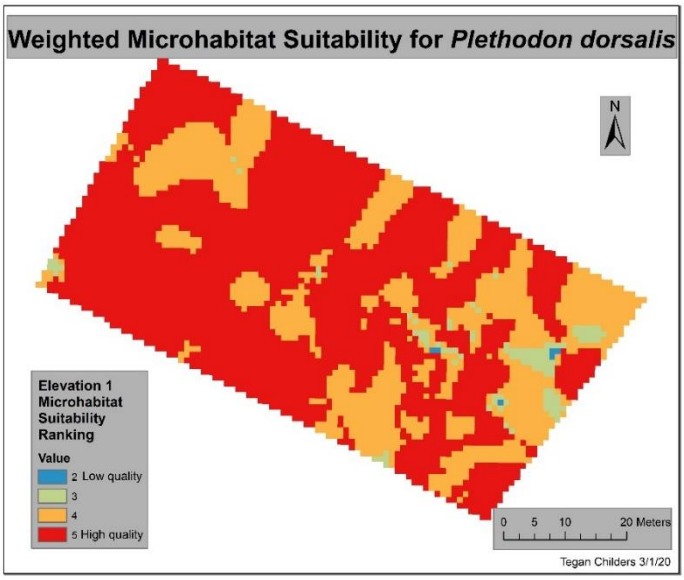

Figure 4.4 Weighted microhabitat suitability model for e1 (Datum: NAD_1983_2011, Coordinate system: StatePlane_ Tennessee_FIPS_4100_Ft_US)

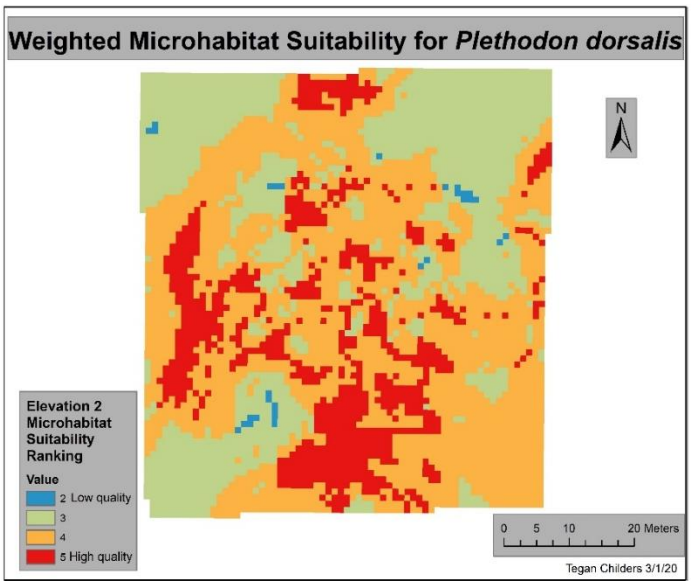

Figure 4.5 Weighted microhabitat suitability model for e2 (Datum: NAD_1983_2011, Coordinate system: StatePlane_ Tennessee_FIPS_4100_Ft_US)

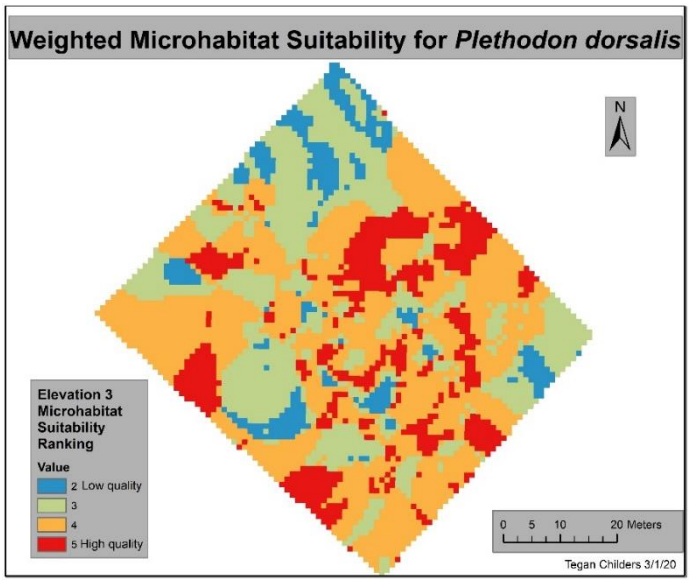

Figure 4.6 Weighted microhabitat suitability model for e3 (Datum: NAD_1983_2011, Coordinate system: StatePlane_ Tennessee_FIPS_4100_Ft_US)

Table 3.1 Counts of pixels for each ranking in the unweighted suitability models

	e1	e1	e2	e2	e3	e3
Ranking	**Count**	**Percent**	**Count**	**Percent**	**Count**	**Percent**
1	23	0.54	211	4.37	79	1.72
2	144	3.39	1220	25.27	1234	26.94
3	1022	24.02	1931	40.00	1795	39.19
4	2215	52.07	1332	27.59	1303	28.45
5	850	19.98	134	2.78	169	3.69
Total count:	4254	4254	4828	4828	4580	4580

Table 3.2 Counts of pixels for each ranking in the weighted suitability models

	e1	e1	e2	e2	e3	e3
Ranking	**Count**	**Percent**	**Count**	**Percent**	**Count**	**Percent**
1	0	0.00	0	0.00	0	0.00
2	6	0.14	30	0.62	395	8.62
3	107	2.52	1574	32.60	1355	29.59
4	1303	30.63	2374	49.17	2059	44.96
5	2838	66.71	850	17.61	771	16.83
Total count:	4254	4254	4828	4828	4580	4580

Table 4.1 Counts of training samples and animal presence points per unweighted model rank

	e1	e1	e2	e2	e3	e3
Ranking	**Count**	**Percent**	**Count**	**Percent**	**Count**	**Percent**
1	0	0.00	0	0.00	2	4.35
2	2	6.45	5	11.63	3	6.52
3	10	32.26	14	32.56	21	45.65
4	15	48.39	16	37.21	10	21.74
5	4	12.90	8	18.60	10	21.74
Total sample points:	31	31	43	43	46	46
Total animal points:	39	39	54	54	57	57

Table 4.2 Counts of training samples and animal presence points per weighted model rank

	e1	e1	e2	e2	e3	e3
Ranking	**Count**	**Percent**	**Count**	**Percent**	**Count**	**Percent**
1	0	0.00	0	0.00	0	0.00
2	0	0.00	0	0.00	0	0.00
3	2	6.45	4	9.30	12	26.09
4	9	29.03	22	51.16	23	50.00
5	20	64.52	17	39.53	11	23.91
Total sample points:	31	31	43	43	46	46
Total animal points:	39	39	54	54	57	57

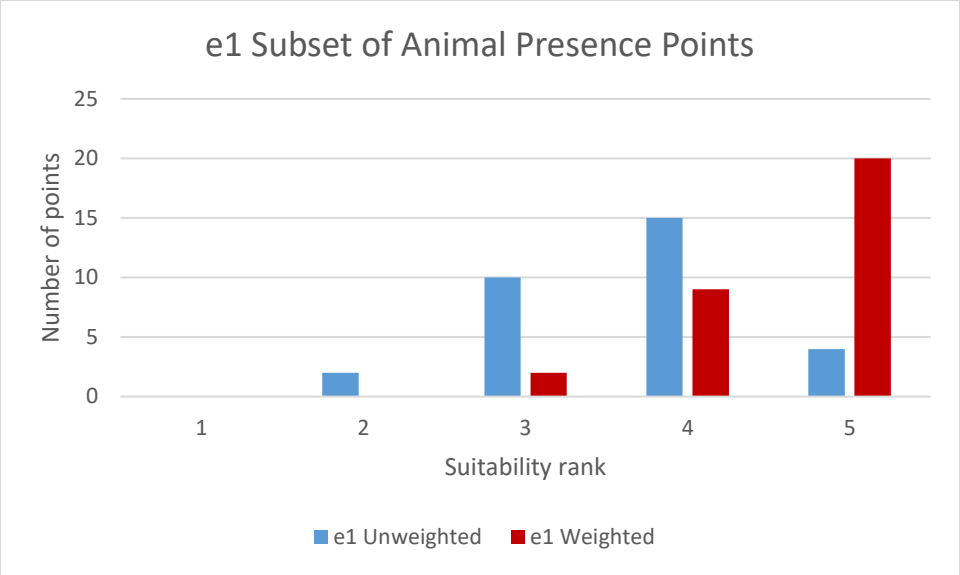

Figure 5.1 Comparison of e1 model counts with animal presence points per model rank

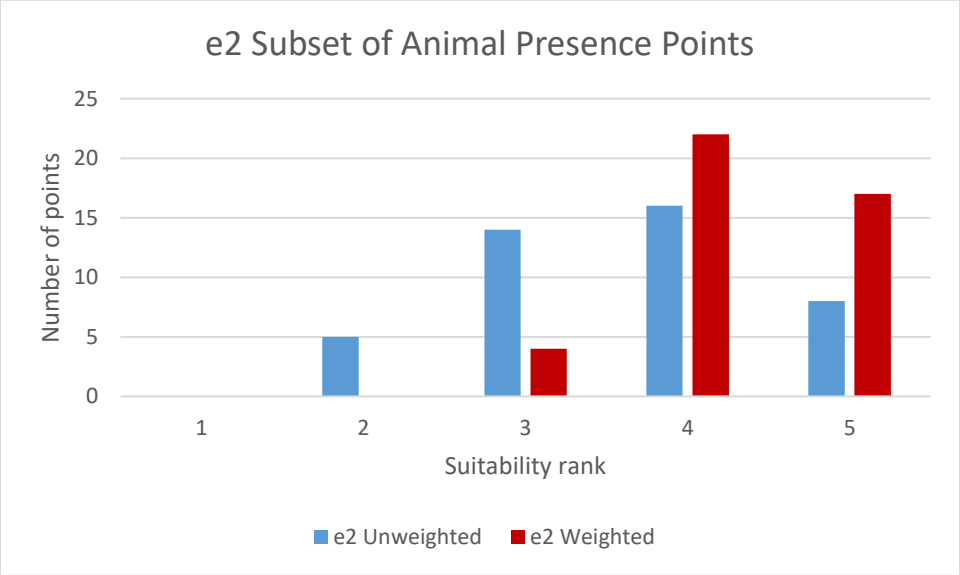

Figure 5.2 Comparison of e2 model counts with animal presence points per model rank

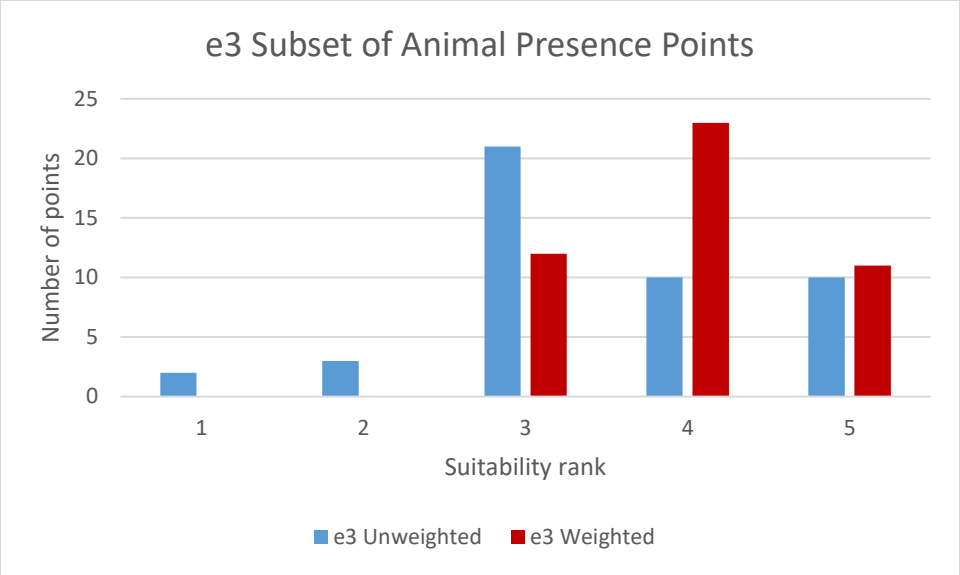

Figure 5.3 Comparison of e3 model counts with animal presence points per model rank

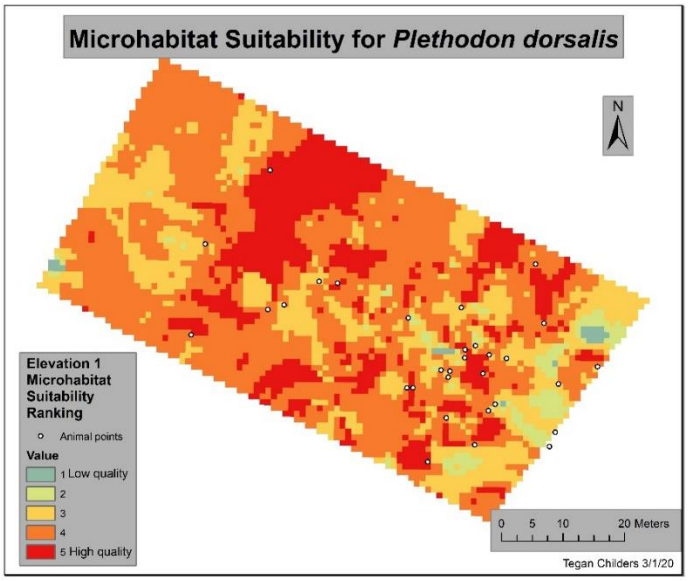

Figure 6.1 Subset of animal presence points with the microhabitat suitability model for e1 (Datum: NAD_1983_2011, Coordinate system: StatePlane_Tennessee_ FIPS_4100_Ft_US)

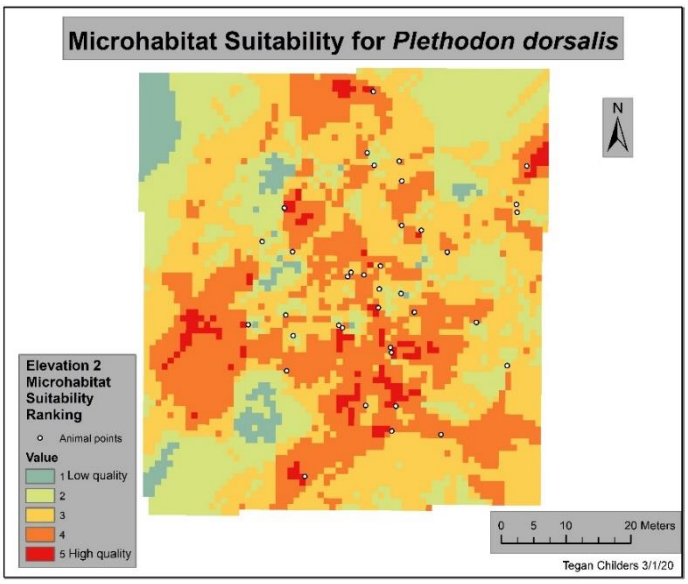

Figure 6.2 Subset of animal presence points with the microhabitat suitability model for e2 (Datum: NAD_1983_2011, Coordinate system: StatePlane_Tennessee_ FIPS_4100_Ft_US)

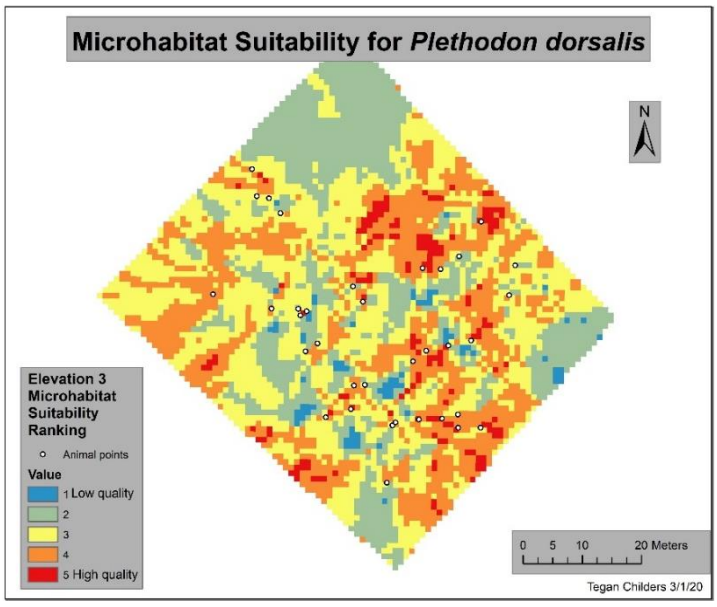

Figure 6.3 Subset of animal presence points with the microhabitat suitability model for e3 (Datum: NAD_1983_2011, Coordinate system: StatePlane_Tennessee_ FIPS_4100_Ft_US)

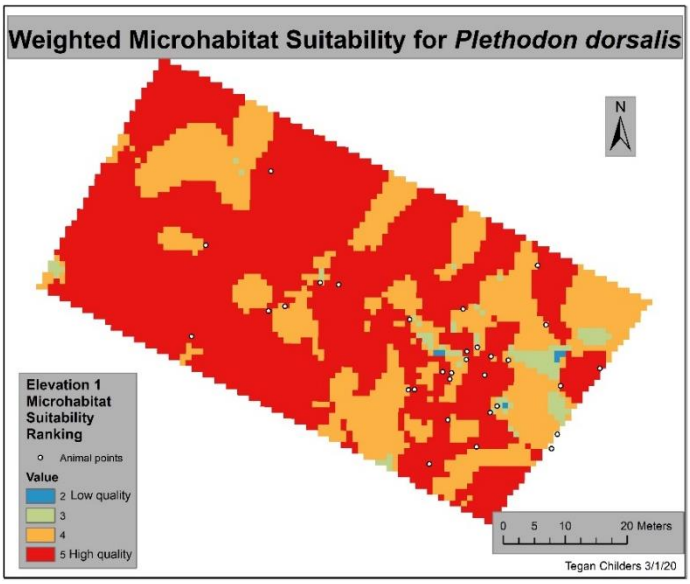

Figure 6.4 Subset of animal presence points with the weighted microhabitat suitability model for e1 (Datum: NAD_1983_2011, Coordinate system: StatePlane_Tennessee_ FIPS_4100_Ft_US)

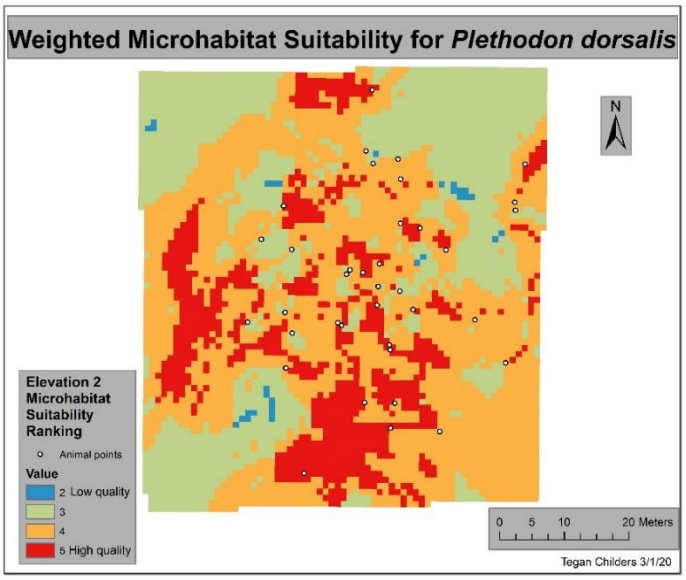

Figure 6.5 Subset of animal presence points with the weighted microhabitat suitability model for e2 (Datum: NAD_1983_2011, Coordinate system: StatePlane_Tennessee_ FIPS_4100_Ft_US)

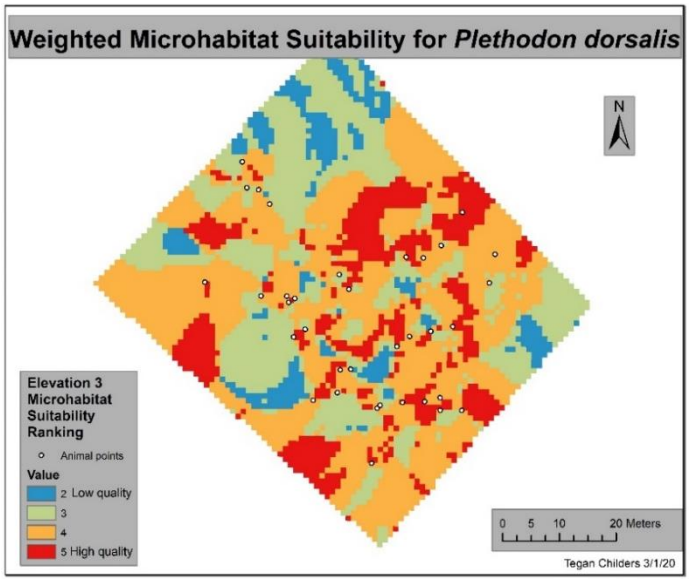

Figure 6.6 Subset of animal presence points with the weighted microhabitat suitability model for e3 (Datum: NAD_1983_2011, Coordinate system: StatePlane_Tennessee_ FIPS_4100_Ft_US)

Discussion

Reflections

Hiking across the varying elevations of the Lower Pot Point Trail, the diversity of habitat structure is apparent at first glance. When comparing the results of the regression analysis to my visual experience acquiring these data, the patterns of habitat preference are understandable. Moving across the survey polygon in e1, there are frequent and thick patches of micro story growth that sometimes resembles carpets of vegetation. Here, I also find little understory development. Opposite of this, in e2, the understory contains many young beech trees and fallen pines propped against living trees; both increasing in number through the year I spent surveying the area. At the highest elevation surveyed, in e3, the canopy was somewhat thinner when compared to other survey polygons. This appeared to be due to older hardwoods and pines

degrading and falling, thereby providing more logs for cover objects. It is generally unsurprising to find that covariates such as rocks and logs were statistically significant in this study. In the majority of cases, salamanders were located under these cover objects. On occasion salamanders are under or near layers of leaf pack and coarse woody debris, but there are usually other logs and rocks within those same quadrats. Patterns like this may be indicative of locating salamanders while they are moving between cover objects. It is also of note, that rocks serve as cover objects less often in e2 and e3 when compared to e1. Visually scanning the area, and excluding the rock wall seen in e1, all three elevations appear to have similar densities of rock distribution. Initially, all three elevations appeared to contain similar distributions of logs as well.

Something that has caught my attention numerous times throughout this process is the general distribution of salamanders. As noted in Tables 5 and 6, the higher elevation shows higher salamander density, and the density decreases with elevation. For the sympatric *P. glutinosus*, there is an inverse density trend.

I do suspect some level of bias in reference to the significance of structures documented as rocks. For example, in e1 there is a manmade barrier composed of rocks. This wall appears to prevent erosion, but it is difficult to search without destroying the structure. It seemed that over time, weather events and falling trees may have dislodged and scattered rocks where I eventually located and documented salamanders. As an alternative to damaging the barrier, I search in between the pockets of rocks and leaf pack to the best of my ability. On a few occasions, I am able to document salamanders in this barrier.

Conclusion

Species Distribution Due to Microhabitat Level Effects

The inverse relationship of species distribution between *P. dorsalis* and *P. glutinosus* is apparent across the elevation gradient of survey polygons. At e3, is the highest density of *P. dorsalis* whereas at e1 there is the highest density of *P. glutinosus*. Contrary to this, all suitability models show that e1 has the greatest amount of suitable microhabitat, with e2 showing less suitable area and e3 showing the least amount of suitable area. Such microhabitat distribution may be a result of resource distribution across the elevation gradient of the TRG. Proximity to roads and trails may also have an effect on salamander distribution. Despite the minimum distance of 50 m from such anthropogenic structures, e1 is still in closer proximity to roads and trails when compared to survey polygons at higher elevations. Increased distance from roads and trails also appeared to minimize accumulation of litter among the survey polygons. However, I strongly suspect that *P. glutinosus* are excluding *P. dorsalis* from accessing certain microhabitat resources. Adult *P. glutinosus* can often weigh over 10 g, but *P. dorsalis* almost never weigh more than 2 g. Cannibalism among salamanders does occur, and is recorded with *P. glutinosus* (Powders, 1973). This may also account for the highest rate of juvenile *P. dorsalis* in e3, and the lowest in e1.

Conservation Implications

Salamanders are bioindicators, decomposers, insectivores, prey for larger animals, and much more. Literature shows that amphibians are exhibiting more significant losses of

biodiversity due to pathogens, deforestation, and climate change than other vertebrate taxa (Baillie, 2004; Blaustein, Walls & Bancroft et al., 2010; Shinwari, Gilani & Kahn, 2012). We know a food web may experience collapse when a key component of high biomass, such as amphibians, disappear. After mass frog mortality events in Panama, there is documentation of decline in the diversity of one of their many predators: snakes (Zipkin, DiRenzo, Ray, Rossman, & Lips, 2020). Overall, the snake population is now small and less diverse because frog-eating snakes now have fewer resources (Zipkin, DiRenzo, Ray, Rossman, & Lips, 2020). Researchers are actively working to understand the broad scale effects of species loss, but there are still many stones left unturned.

Proactive habitat management is key when facing the swift loss of any taxa (Shoo, Olson & McMenamin, 2011). Continued acquisition of macrohabitat scale data only strengthens the best management practices of federal, state and non-government land managers. Prior to this study, the limited research done with *P. dorsalis* focuses on ex situ data. These studies include the aforementioned genetic work, honing in on structural differences (Server, 1978a; Server, 1978b) and courtship methods (Picard, 2005) of the species when compared to its sister taxa. Scientists still have much to learn about *P. dorsalis*; this methodology and these data provide a template for expanding our knowledge of this species. Statistically significant data such as these are evidence of preference for particular cover objects and microhabitat components.

Knowledge of microhabitat data carry large conservation implications. Understanding how to improve upon best land management practices means knowing how to improve the health of an ecosystem. As discussed earlier in this document, salamanders are contributors to the nutrient cycle. Functioning as decomposers, consumers of invertebrates, and prey items for larger animals, these individuals play a significant role in a balanced ecosystem. To ensure the

opportunity for salamanders to exist in a landscape is to encourage the health of an ecosystem. Based upon the statistically significant data in this document, it is clear that the practice of leaving branches and down trees where they fall can contribute to ideal *P. dorsalis* habitat. Actions, or rather inactions, like not disturbing rocks or layers of leaf litter can also assist in improving habitat for these salamanders.

Future Directions

Compared to the 200 m buffer of the Lower Pot Point Trail, the expanse of the TRG is vast. It is beneficial to increase the number of polygons surveyed to increase the overall comprehension habitat variability in the TRG. Sampling on the opposite side of the TRG while continuing to sample across the same elevation gradient should be included as well to identify variation between the two sets of slopes. The covariate boulder needs further assessment. During ground-truthing efforts to investigate land cover qualities, as discussed in chapter one, it was apparent that boulders are not frequently distributed across all slopes within the 200 m buffer around the trail. Though there are many boulders across the elevation gradient, the only survey polygon containing a boulder was e1. Boulders were visible from the polygons at e2 and e3 as well. There is also a rock climbing community in the area that occasionally uses these boulders for climbing and recreation. Though unintended by the climbers, they most likely alter potential salamander microhabitat when they recreate in the area. Taking this into consideration, future sampling should cover a wide variety of boulder sizes and locations, if possible.

Methodology described in this document provides a clear path to streamline survey methods for quantifying the habitat preference of *P. dorsalis*, and possibly its sister taxa as well.

To establish better comprehension of terrestrial salamander microhabitat preferences, I suggest the utilization of tools described in this document.

REFERENCES

Akaike, H. (1973). Information Theory and an Extension of the Maximum Likelihood Principle. In E. Parzen, K. Tanabe, & G. Kitagawa (Eds.), *Selected Papers of Hirotugu Akaike* (pp. 199-213). New York, NY: Springer New York.

Baillie, J. E.M. (2004). 2004 IUCN Red List of Threatened Species: A Global Species Assessment. *The IUCN Species Survival Commission*.

Blaustein, A. R., Walls, S. C., Bancroft, B. A., Lawler, J. J., Searle, C. L., & Gervasi, S. S. (2010). Direct and indirect effects of climate change on amphibian populations. *Diversity, 2*(2), 281-313. doi:10.3390/d2020281

Blyveis, E. R. (2011). *The Vascular Flora of the Tennessee River Gorge, Hamilton and Marion Counties, Tennessee.* (Master of Environmental Science), University of Tennessee at Chattanooga, Chattanooga, Tennessee.

Bonissone, P. P., Subbu, R., & Lizzi, J. (2009). Multicriteria decision making (MCDM): a framework for research and applications. IEEE Computational Intelligence Magazine, 4(3), 48-61.

Briggler, J. T., & Puckette, W.L. (2003). Observations on reproductive biology and brooding behavior of the Ozark Zigzag Salamander, Plethodon angusticlavius. *The Southwestern Naturalist, 48*(1), 96-100.

Britton, J. M. (1981). Microhabitat distribution and its effect of prey utilization in sympatric populations of Plethodon glutinosus and Plethodon dorsalis in Northwestern Arkansas. *Journal of the Arkansas Academy of Science, 35*.

Burton, T. M., & Likens, G. E. (1975). Salamander populations and biomass in the Hubbard Brook experimental forest, New Hampshire. *Copeia*, 541-546.

Carver, S. J. (1991). Integrating multi-criteria evaluation with geographical information systems. *International Journal of Geographical Information System*, 5(3), 321-339.

Compton, B. W., Rhymer, J. M., & McCollough, M. J. E. (2002). Habitat selection by wood turtles (Clemmys insculpta): An application of paired logistic regression. *Ecology, 83*(3), 833-843.

Davic, R. D., & Welsh, H. H. (2004). On the ecological roles of salamanders. *Annual Review of Ecology, Evolution, and Systematics, 35*(1), 405-434. doi:10.1146/annurev.ecolsys.35.112202.130116

Dillard, L. O., Russell, K. R., & Ford, W. M. (2008). Site-level habitat models for the endemic, threatened Cheat Mountain salamander (Plethodon nettingi): the importance of geophysical and biotic attributes for predicting occurrence. *Biodiversity and Conservation, 17*(6), 1475-1492. doi:10.1007/s10531-008-9356-x

Dodd, C. K. (2010). *Amphibian ecology and conservation: a handbook of techniques*. 198 Madison Avenue, New York, New York 10016: Oxford University Press.

Dupuis, L. A., Smith, J. N., & Bunnell, F. (1995). Relation of terrestrial-breeding amphibian abundance to tree-stand age. *Conservation Biology,* 9(3), 645-653.

Explorer, N. S. (2002). Plethodon dorsalis: Northern Zigzag Salamander. Retrieved from http://explorer.natureserve.org/servlet/NatureServe?searchName=Plethodon+dorsalis

Farallo, V. R., & Miles, D. B. (2016). The Importance of Microhabitat: A Comparison of two microendemic species of Plethodon to the widespread P. cinereus. *Copeia, 104*(1), 67-77. doi:10.1643/ce-14-219

Groff, L. A., Calhoun, A. J., & Loftin, C. S. (2016). Hibernal habitat selection by wood frogs (Lithobates sylvaticus) in a northern New England montane landscape. *Journal of Herpetology, 50*(4), 559-569.

Grover, M. C. (1998). Influence of cover and moisture on abundances of the terrestrial salamanders Plethodon cinereus and Plethodon glutinosus. *Journal of Herpetology, 32*(4), 489-497.

Gustafson, E. J., Murphy, N. L., & Crow, T. R. (2001). Using a GIS model to assess terrestrial salamander response to alternative forest management plans. *Journal of Environmental Management, 63*(3), 281-292.

Highton, R. (1997). Geographic protein variation and speciation in the Plethodon dorsalis Complex. *Herpetologica, 53*(3), 345-356.

Highton, R. (1999). Geographic protein variation and speciation in the salamanders of the Plethodon cinereus group with the description of two new species. *Herpetologica, 55*(1), 43-90.

Highton, R., Hastings, A. P., Palmer, C., Watts, R., Hass, C. A., Culver, M., & Arnold, S. J. (2012). Concurrent speciation in the eastern woodland salamanders (Genus Plethodon): DNA sequences of the complete albumin nuclear and partial mitochondrial 12s genes. *Mol Phylogenet Evol, 63*(2), 278-290. doi:10.1016/j.ympev.2011.12.018

Jaeger, R. G. (1979). Seasonal spatial distributions of the terrestrial salamander Plethodon cinereus. *Herpetologica, 35*(1), 90-93.

Kern, M. M., Nassar, A. A., Guzy, J. C., & Dorcas, M. E. (2013). Oviposition site selection by Spotted salamanders (Ambystoma maculatum) in an isolated Wetland. *Journal of Herpetology, 47*(3), 445-449. doi:10.1670/11-179.

Kleeberger, S. R., & Werner, J. K. (1982). Home range and homing behavior of Plethodon cinereus in northern Michigan. *Copeia*, 409-415.

Larson, A., & Highton, R. (1978). Geographic protein variation and divergence in the salamanders of the Plethodon weller group (Amphibia, Plethodontidae). *Systematic Zoology, 27*(4), 431-448.

Marsh, D. M. & Goicochea, M. A. (2003). Monitoring terrestrial salamanders: Biases caused by intense sampling and choice of cover objects. *Journal of Herpetology, 37*(3), 460-466.

Mathis, A., Deckard, K., & Duer, C. (1998). Laboratory evidence for territorial behavior by the southern red-backed salamander, Plethodon serratus: influence of residency status and pheromonal advertisement. *The Southwestern Naturalist, 43*(1), 1-5.

Mueller, R. L., Macey, J. R., Jaekel, M., Wake, D. B., & Boore, J. L. (2004). Morphological homoplasy, life history evolution, and historical biogeography of plethodontid salamanders inferred from complete mitochondrial genomes. *Proceedings of the National Academy of Sciences, 101*(38), 13820-13825.

Niemiller, M. L., & Reynolds, R. G. (2011). *The amphibians of Tennessee*. Knoxville, Tennessee: University of Tennessee Press.

Petranka, J. W. (1998). *Salamanders of the United States and Canada*. Washington: Smithsonian Institution Press.

Picard, A. L. (2005). Courtship in the Zig-Zag Salamander (Plethodon dorsalis): Insights into a transition in Pheromone-delivery behavior. *Ethology, 111*(9), 799-809.

Powell, R., Conant, R., & Collins, J. T. (2016). *Peterson field guide to reptiles and amphibians of eastern and central North America*. 3 Park Avenue, 19th Floor, New York, New York 10016: Houghton Mifflin Harcourt.

Powders, V. N. (1973). Cannibalism by the slimy salamander, Plethodon glutinosus in eastern Tennessee. *Journal of Herpetology*, 7(2), 139-140.

Price, S. J., Eskew, E. A., Cecala, K. K., Browne, R. A., & Dorcas, M. E. (2012). Estimating survival of a streamside salamander: importance of temporary emigration, capture response, and location. *Hydrobiologia, 679*(1), 205-215.

Roe, A. W., & Grayson, K. L. (2008). Terrestrial movements and habitat use of juvenile and emigrating adult eastern red-spotted newts, Notophthalmus viridescens. *Journal of Herpetology*, *42*(1), 22-30.

Rozenstein, O., & Karnieli, A. (2011). Comparison of methods for land-use classification incorporating remote sensing and GIS inputs. *Applied Geography, 31*(2), 533-544.

Schieltz, J. M., Haywood, L. M., & Marsh, D. M. (2010). Effects of cover object spacing on the socioecology of the red-backed salamander, Plethodon cinereus. *Herpetologica, 66*(3), 276-282.

Semlitsch, R. D., O'Donnell, K. M., & Thompson, F. R. (2014). Abundance, biomass production, nutrient content, and the possible role of terrestrial salamanders in Missouri Ozark forest ecosystems. *Canadian Journal of Zoology, 92*(12), 997-1004. doi:10.1139/cjz-2014-0141

Sever, D. M. (1978a). Female cloacal anatomy of Plethodon cinereus and Plethodon dorsalis (Amphibia, Urodela, Plethodontidae). *Journal of Herpetology*, 397-406.

Sever, D. M. (1978b). Male cloacal glands of Plethodon cinereus and Plethodon dorsalis (Amphibia: Plethodontidae). *Herpetologica*, 1-20.

Shoo, L. P., Olson, D. H., McMenamin, S. K., Murray, K. A., Van Sluys, M., Donnelly, M. A., Stratford, D., Terhivuo, J., Merino-Viteri, A., Herbert, S. M., Bishop, P. J., Corn, P. S., Dovey, L., Griffiths R. A., Lowe, K., Mahony, M., McCallum, H., Shuker, J. D., Simpkins, C., . . . Hero, J.-M. (2011). Engineering a future for amphibians under climate change. *Journal of Applied Ecology, 48*(2), 487-492. doi:10.1111/j.1365-2664.2010.01942.x

Smith, A. M., & Green, M. D. (2005). Dispersal and the metapopulation paradigm in amphibian ecology and conservation: Are all amphibian populations metapopulations? *Ecography, 28*(1), 110-128.

Thurow, G. R. (1956). Comparisons of two species of salamanders, Plethodon cinereus and Plethodon dorsalis. *Herpetologica*, *12*(3), 177-182.

Thurow, G. R. (1957). Relationships of the red-backed and zigzag plethodons in the west. *Herpetologica*, *13*(2), 91-99.

Weih, R. C., & Riggan, N. D. (2010). Object-based classification vs. pixel-based classification: comparative importance of multi-resolution imagery. *The International Archives of the Photogrammetry, Remote Sensing and Spatial Information Sciences, 38*(4), C7.

Youngman, H. (2017). *Post-fledging habitat use and movements of worm-eating warblers in the Tennessee River Gorge.* (Master of Environmental Science), University of Tennessee at Chattanooga, Chattanooga, Tennessee.

Shinwari, Z.K., Gilani, S. A. & Kahn, A. L. (2012). Biodiversity loss, emerging infectious diseases and impact on human and crops. *Pakistan Journal of Botany, 44*, 137-142.

Zipkin, E. F., DiRenzo, G. V., Ray, J. M., Rossman, S., & Lips, K. R. (2020). Tropical snake diversity collapses after widespread amphibian loss. *Science*, *367*(6479), 814-81

APPENDIX A

SAS CODE FOR PROC UNIVARIATE AND PROC LOGISTIC STATEMENTS

```
PROC IMPORT OUT= WORK.Tegan_e1T
            DATAFILE= "E:\Dorsalis conditional matched pairs regression.xlsx"
            DBMS=EXCEL REPLACE;
     RANGE="e1T$";
     GETNAMES=YES;
     MIXED=NO;
     SCANTEXT=YES;
     USEDATE=YES;
     SCANTIME=YES;
RUN;
Proc logistic data=Tegan_e1T;
model anim_pres (event='1')=soil_surface_temp__F microstory leaflitter moss
wdybr cwd logs rocks;
run;
proc univariate data=Tegan_e1T;
   var soil_surface_temp__F microstory leaflitter moss wdybr cwd logs rocks;
   histogram soil_surface_temp__F microstory leaflitter moss wdybr cwd logs
rocks;
run;
```

APPENDIX B

PYTHON SCRIPT DEVELOPED FOR BOX COX TRANSFORMATION AND TRANSFORMED OUTPUTS USED IN SAS

```
import pandas as pd
from scipy import stats
df = pd.read_csv("test4.csv")
'''for row in df.loc:
    print(row)
    row1 = row[2:]
    cleanrow = row1.add(1).astype(float)
    boxcox = stats.boxcox(cleanrow)
    print(boxcox)'''
row1 = df.loc[6, 'id_field':] #this is the only row that you should edit anything in!
Change the number
print(row1)
cleanrow = row1.add(1).astype(float)
print(cleanrow)
boxcox = stats.boxcox(cleanrow)
print(boxcox)
```

Table 5.1 Transformed data output for e1, The abbreviation for coarse woody debris is CWD.

Date	ID	Microstory	Leaflitter	Moss	Woody Brush	CWD	Logs	Rocks
11/10/2018	e1_a1	1.37939389	9.62E+05	0.21047	0	1.71427739	0	0.46495227
11/10/2018	e1_a1_rp	1.50408045	9.62E+05	0.58024	0	1.59407904	0	0
11/10/2018	e1_b1	1.2394084	5.84E+05	1.0834	0	0.66212645	0.80919215	0
11/10/2018	e1_b1_rp	0.71817806	1.34E+06	0	0	1.02204742	0	0
11/10/2018	e1_a2	1.5998248	7.08E+05	0.21047	0	1.15386573	0.7870692	0
11/10/2018	e1_a2_rp	1.37939389	1.24E+06	0	0	0.39471568	0	0
11/10/2018	e1_a3	0.71817806	1.03E+06	1.15756	0	0.86260693	0	0.575865
11/10/2018	e1_a3_rp	0.51433829	1.17E+06	0	0	1.76728036	0	0
11/23/2018	e1_a4	1.20556003	9.44E+05	0.58024	0	1.31609013	0.72194913	0.42756326
11/23/2018	e1_a4_rp	0.93306788	9.26E+05	1.03716	0	1.44869344	0	0.5986137
11/23/2018	e1_a6	1.53858437	7.35E+04	1.42213	0.41738802	2.59131132	0.80705654	0
11/23/2018	e1_a6_rp	2.06242885	5.29E+05	0	0.35780827	0.66212645	0	0
11/23/2018	e1_b2	0.62459413	9.35E+05	0.58024	0	0.76868907	0.78980143	0
11/23/2018	e1_b2_rp	0.51433829	1.45E+06	0	0	0.21986157	0	0
11/23/2018	e1_b3	0.62459413	1.30E+06	0.83312	0	0.76868907	0	0
11/23/2018	e1_b3_rp	1.12985586	8.32E+05	0.83312	0	1.62615034	0.75557895	0
12/7/2018	e1_a7	0.62459413	9.44E+05	0.48436	0	0.76868907	0.78980143	0
12/7/2018	e1_a7_rp	0.51433829	1.45E+06	0	0	0.21986157	0	0
12/7/2018	e1_a8	0.87005596	1.39E+06	0	0	0.39471568	0	0
12/7/2018	e1_a8_rp	0.62459413	1.30E+06	0.91589	0	0.21986157	0	0.30225602
12/7/2018	e1_a9	0.71817806	1.31E+06	0.65937	0	0.21986157	0	0.46495227
12/7/2018	e1_a9_rp	0.71817806	1.27E+06	0.21047	0	1.31609013	0	0
12/7/2018	e1_a10	0.62459413	1.09E+06	0.21047	0	0.53927728	0.76767181	0
12/7/2018	e1_a10_rp	1.94091302	6.30E+05	0	0	1.59407904	0	0
12/7/2018	e1_a11	0.62459413	1.08E+06	0.83312	0	0.21986157	0	0.62112281
12/7/2018	e1_a11_rp	0.93306788	8.08E+05	1.29895	0	1.44869344	0	0
12/14/2018	e1_a10.1	0.21569836	6.79E+05	1.26096	0.44560317	1.59407904	0.73899754	0
12/14/2018	e1_a10.1_rp	0.79908204	1.28E+06	0	0	1.26588558	0	0
12/14/2018	e1_a11.1	1.16916246	8.65E+05	0.36492	0	0.39471568	0	0.63991677
12/14/2018	e1_a11.1_rp	0.93306788	7.15E+05	1.33099	0	1.59407904	0.7150101	0
12/14/2018	e1_a12.1	0.21569836	1.36E+06	0	0	1.15386573	0	0
12/14/2018	e1_a12.1_rp	0.62459413	1.45E+06	0	0	0	0	0
12/21/2018	e1_b4	0.38132888	1.31E+06	0	0	1.36305457	0	0
12/21/2018	e1_b4_rp	1.69921227	9.44E+05	0	0	1.26588558	0	0
12/21/2018	e1_a13	0.21569836	9.89E+05	0.91589	0.4501336	1.26588558	0	0.42756326
12/21/2018	e1_a13_rp	1.30060664	1.25E+06	0	0	0.66212645	0	0
12/30/2018	e1_a14	0.51433829	8.49E+05	0	0	2.31842895	0	0
12/30/2018	e1_a14_rp	0.79908204	3.34E+05	1.45403	0	1.26588558	0	0.64670591
12/30/2018	e1_a15	0.21569836	5.72E+05	1.48036	0	1.59407904	0	0.575865
12/30/2018	e1_a15_rp	0.93306788	1.39E+06	0	0	0.21986157	0	0
12/30/2018	e1_a16	0.21569836	1.10E+06	1.03716	0	1.59407904	0	0
12/30/2018	e1_a16_rp	0.51433829	1.15E+06	0.58024	0	1.71427739	0	0
12/30/2018	e1_a17	0.62459413	1.17E+06	1.0834	0	1.09083166	0	0
12/30/2018	e1_a17_rp	0.51433829	9.89E+05	0	0	0.66212645	0.78980143	0

1/25/2019	e1_a18	0.62459413	1.16E+06	0	0	1.26588558	0	0.5888335
1/25/2019	e1_a18_rp	0.93306788	1.12E+06	0.21047	0.26935051	1.26588558	0.32142099	0.53240177
2/2/2019	e1_a19	1.12985586	8.57E+05	1.03716	0	1.44869344	0.73899754	0
2/2/2019	e1_a19_rp	1.27100683	7.76E+05	0.98233	0.4501336	1.71427739	0	0
2/2/2019	e1_a20	1.27100683	8.57E+05	0.36492	0.4501336	1.26588558	0	0.575865
2/2/2019	e1_a20_rp	1.04066505	1.20E+06	0	0	1.44869344	0	0
2/2/2019	e1_a21	1.12985586	5.05E+05	1.43889	0	1.02204742	0.7150101	0.61222858
2/2/2019	e1_a21_rp	1.12985586	7.45E+05	0.98233	0.44560317	1.02204742	0.76767181	0
2/2/2019	e1_a22	0.62459413	7.92E+05	0.83312	0.26935051	1.02204742	0.79845172	0
2/2/2019	e1_a22_rp	0.93306788	1.15E+01	0.98233	0	1.26588558	0	0
3/1/2019	e1_a18.1	0.93306788	6.17E+05	1.31562	0.17675754	0.53927728	0	0.64160908
3/1/2019	e1_a18.1_rp	0.71817806	1.27E+06	0.21047	0.38079002	0.86260693	0	0.30225602
3/1/2019	e1_a18.2	1.16916246	9.17E+05	0.48436	0	0.66212645	0.78065052	0.18908843
3/1/2019	e1_a18.2_rp	1.66493058	8.82E+05	0	0	1.65679986	0	0
3/23/2019	e1_a25	1.53858437	8.32E+05	1.0834	0.35780827	1.09083166	0	0.53240177
3/23/2019	e1_a25_rp	1.27100683	1.18E+06	0	0.35780827	1.02204742	0	0
3/23/2019	e1_a26	1.37939389	9.44E+05	1.0834	0	0.66212645	0	0.575865
3/23/2019	e1_a26_rp	1.12985586	6.86E+05	0.58024	0.44560317	1.59407904	0.77685041	0
3/23/2019	e1_a27	1.37939389	9.44E+05	1.0834	0	0.66212645	0	0.575865
3/23/2019	e1_a27_rp	1.5998248	1.02E+06	0	0.35780827	1.02204742	0	0
3/23/2019	e1_b7	1.12985586	9.44E+05	1.0834	0.35780827	1.02204742	0	0.575865
3/23/2019	e1_b7_rp	1.27100683	1.13E+06	0.58024	0.35780827	1.02204742	0	0
3/23/2019	e1_a28	1.46643398	7.15E+05	0.98233	0.4501336	1.44869344	0	0.53240177
3/23/2019	e1_a28_rp	1.53858437	4.19E+05	0.83312	0.35780827	1.02204742	0.81553597	0
3/23/2019	e1_b8	1.12985586	3.43E+05	1.29895	0.41738802	1.59407904	0.80919215	0.53240177
3/23/2019	e1_b8_rp	1.27100683	2.77E+05	0.58024	0.43695469	2.05281892	0.81553597	0.53240177
3/29/2019	e1_a29	1.04066505	1.08E+06	0.48436	0.35780827	1.26588558	0	0.53240177
3/29/2019	e1_a29_rp	1.35463104	1.16E+06	0	0.17675754	1.15386573	0	0
3/29/2019	e1_a30	1.12985586	5.84E+05	0.21047	0.17675754	2.13047648	0.78980143	0
3/29/2019	e1_a30_rp	1.62720625	8.49E+05	0.48436	0	1.52513515	0	0.53240177
4/7/2019	e1_a31	1.37939389	6.30E+05	0.98233	0	1.59407904	0.78980143	0
4/7/2019	e1_a31_rp	1.12985586	1.22E+06	0.58024	0.35780827	0.66212645	0	0
4/7/2019	e1_b9	1.37939389	9.44E+05	0.58024	0	1.81642254	0	0
4/7/2019	e1_b9_rp	0.93306788	1.13E+06	0	0.41738802	1.44869344	0	0
Lambda Value =		-0.305888079	3.3421607	-0.52916	-2.176590707	-0.13313366	-1.193823624	-1.527602458

Table 5.2 Transformed data output for e2. The abbreviation for coarse woody debris is CWD.

Date	ID	Microstory	Leaflitter	Moss	Woody brush	CWD	Logs	rocks
11/4/2018	e2_a1	0.9838313	1.15E+01	0.43520151	0.24000437	1.89470902	0.80485386	0.40771782
11/4/2018	e2_a1_rp	2.83169877	9.20E+02	0	0.23766705	2.02104325	0	0
12/8/2018	e2_a10	1.7695065	5.73E+03	0	0	3.57303168	0	0
12/8/2018	e2_a10_rp	1.99541006	1.32E+04	0	0	2.77837149	0	0
12/8/2018	e2_a11	2.60084286	7.19E+03	0	0	1.74828819	0	0
12/8/2018	e2_a11_rp	0.52874921	2.66E+04	0.17570654	0	0.68657594	0	0.39574762
12/16/2018	e2_a12	1.99541006	1.28E+04	0	0	2.82826625	0	0
12/16/2018	e2_a12_rp	1.69347841	1.46E+04	0	0.23984744	2.66942051	0	0
12/16/2018	e2_a13	2.03891364	1.07E+04	0	0	3.00398377	0	0
12/16/2018	e2_a13_rp	1.20693618	1.88E+04	0.38973168	0	0.80194568	0.83082909	0.3816041
12/16/2018	e2_a14	2.11565372	9.21E+03	0	0	1.57430514	0.86203403	0
12/16/2018	e2_a14_rp	2.18162371	7.51E+03	0.35240268	0	1.36017527	0	0.40946109
12/16/2018	e2_a15	1.89488946	1.19E+04	0	0	3.00398377	0	0
12/16/2018	e2_a15_rp	0.52874921	1.80E+04	0	0	2.18294909	0.83082909	0
12/16/2018	e2_a16	1.60503816	2.30E+03	0.44536154	0	3.41243488	0	0.40916521
12/16/2018	e2_a16_rp	0	2.21E+04	0	0	2.47648874	0	0
12/16/2018	e2_a17	0	1.99E+03	0	0	3.6905925	0.86203403	0
12/16/2018	e2_a17_rp	1.37116405	2.48E+04	0	0	1.52520016	0	0
12/16/2018	e2_a18	0.64621336	2.46E+04	0.40905337	0	1.36017527	0	0.3816041
12/16/2018	e2_a18_rp	0.9838313 0.747192	2.66E+04	0	0	1.36017527	0	0
12/16/2018	e2_a19	0.52874921	2.64E+04	0	0	1.57430514	0	0
12/16/2018	e2_a19_rp	0.64621336	1.80E+04	0	0	2.18294909	0.83082909	0
11/4/2018	e2_a2	2.62300306	2.46E+04	0.40905337	0	1.36017527	0	0.3816041
11/4/2018	e2_a2_rp	2.64395501	5.80E+03	0.31934653	0.23766705	1.36017527	0	0.3816041
12/16/2018	e2_a20	1.4998891	2.63E+03	0	0	2.92043037	0	0
12/16/2018	e2_a20_rp	0.64621336	5.73E+03	0	0	3.63378299	0	0
12/22/2018	e2_a21	0.9838313	2.27E+04	0	0	2.32046496	0	0
12/22/2018	e2_a21_rp	1.15802188	1.66E+04	0	0	2.13209312	0.8411666	0
12/22/2018	e2_a22	0.52874921	1.40E+04	0.42024812	0	1.0821657	0.86203403	0
12/22/2018	e2_a22_rp	0.64621336	1.80E+04	0	0	2.18294909	0.83082909	0
12/22/2018	e2_a23	1.69347841	2.07E+04	0	0	1.47336447	0.83082909	0
12/22/2018	e2_a23_rp	0.52874921	2.63E+03	0.44684666	0.23939535	2.66942051	0.86352308	0
12/22/2018	e2_a24	1.43905535	2.76E+04	0.17570654	0	1.0821657	0	0.25739714
12/22/2018	e2_a24_rp	0.83548021	2.49E+04	0	0	1.36017527	0	0
12/22/2018	e2_a25	2.21137802	1.90E+04	0.35240268	0	1.57430514	0.83645473	0
12/22/2018	e2_a25_rp	0.2181234	1.03E+04	0	0	1.89470902	0.70314191	0.40815287
1/5/2019	e2_a26	1.60503816	2.78E+04	0.40905337	0	0	0	0.33420916
1/5/2019	e2_a26_rp	0.64621336	8.85E+03	0.40905337	0	3.21593946	0	0.40158085
1/5/2019	e2_a27	0.38909282	2.15E+04	0	0	2.47648874	0	0
1/5/2019	e2_a27_rp	1.67266923	2.68E+04	0	0	1.62094949	0	0
1/5/2019	e2_a28	0.2181234	1.99E+04	0.35240268	0	1.86022101	0	0.38657961
1/5/2019	e2_a28_rp	0.747192	2.05E+04	0	0	1.47336447	0.83645473	0
1/5/2019	e2_a29	1.37116405	1.92E+04	0.35240268	0	2.65482627	0	0
1/5/2019	e2_a29_rp	1.67266923	3.18E+03	0	0	3.84173261	0	0

11/4/2018	e2_a3	1.7695065	1.99E+04	0.35240268	0	1.86022101	0	0.38657961
11/4/2018	e2_a3_rp	1.20693618	1.66E+04	0	0.23939535	1.0821657	0.82400274	0
1/5/2019	e2_a30	1.7695065	2.27E+04	0	0	1.57430514	0	0.40158085
1/5/2019	e2_a30_rp	0.38909282	1.98E+04	0	0	1.89470902	0	0.3816041
1/21/2019	e2_a31	0.38909282	2.48E+04	0.17570654	0.23984744	1.36017527	0	0
1/21/2019	e2_a31_rp	0	2.69E+04	0	0	1.57430514	0	0
1/21/2019	e2_a32	0.9838313	1.19E+04	0.40905337	0	3.15074267	0	0.40158085
1/21/2019	e2_a32_rp	0.83548021	2.09E+04	0	0	1.89470902	0.7908802	0
1/21/2019	e2_a33	0.9838313	2.78E+04	0	0	0.99764525	0	0
1/21/2019	e2_a33_rp	1.52805836	1.61E+04	0	0.24011692	2.47648874	0	0.33420916
1/21/2019	e2_a34	1.7695065	1.80E+04	0.35240268	0.14531878	2.27688871	0	0.39765819
1/21/2019	e2_a34_rp	1.37116405	1.37E+04	0	0	2.92043037	0	0
1/21/2019	e2_a35	1.4998891	2.61E+04	0	0.14531878	0.90483094	0	0
1/21/2019	e2_a35_rp	0.64621336	1.71E+04	0.35240268	0	2.66942051	0	0
1/27/2019	e2_a36	1.60503816	2.40E+04	0	0	2.13209312	0	0
1/27/2019	e2_a36_rp	0.52874921	1.28E+04	0	0	2.66942051	0.82400274	0
1/27/2019	e2_a37	2.70930569	1.44E+04	0.43520151	0	2.45838963	0.83082909	0
1/27/2019	e2_a37_rp	0.64621336	1.34E+03	0	0	2.82826625	0	0.40158085
1/27/2019	e2_a38	1.83597982	2.40E+04	0	0	2.13209312	0	0
1/27/2019	e2_a38_rp	0.9838313	1.15E+04	0	0	2.60957148	0.83082909	0
1/27/2019	e2_a39	1.99541006	1.88E+04	0.26665316	0.2267481	1.41848122	0.83082909	0.33420916
1/27/2019	e2_a39_rp	0.38909282	2.09E+04	0	0	1.0821657	0	0
11/4/2018	e2_a4	1.8037973	2.15E+04	0	0	2.51163789	0	0
11/4/2018	e2_a4_rp	0.9838313	1.30E+04	0	0	2.96318301	0	0
1/27/2019	e2_a40	0.64621336	2.53E+04	0	0	1.74828819	0	0
1/27/2019	e2_a40_rp	1.20693618	4.95E+03	0	0	1.36017527	0.88025135	0
1/27/2019	e2_a41	1.69347841	2.59E+04	0	0.14531878	1.2979981	0	0
1/27/2019	e2_a41_rp	0.38909282	1.63E+04	0.42727093	0	1.66536522	0.81555655	0
2/24/2019	e2_a42	1.37116405	2.15E+04	0	0	2.51163789	0	0
2/24/2019	e2_a42_rp	1.10501191	1.61E+04	0	0	1.89470902	0.84516752	0
2/24/2019	e2_a43	1.4998891	2.46E+04	0	0	1.82439473	0	0
2/24/2019	e2_a43_rp	1.69347841	1.98E+04	0	0	1.36017527	0	0.40771782
2/24/2019	e2_a44	1.99541006	2.09E+04	0	0	2.02104325	0	0
2/24/2019	e2_a44_rp	0.83548021	4.70E+03	0	0	2.02104325	0.87532087	0
3/24/2019	e2_a45	1.4998891	2.66E+04	0	0.21678576	1.23140727	0.1974033	0
3/24/2019	e2_a45_rp	0.83548021	1.98E+04	0	0	1.36017527	0	0.40771782
3/24/2019	e2_a46	2.21137802	2.49E+04	0	0	1.89470902	0	0
3/24/2019	e2_a46.1	1.60503816	1.32E+04	0	0	2.40182065	0	0
3/24/2019	e2_a46.1_rp	1.73284009	1.24E+04	0	0	2.47648874	0.84516752	0
3/24/2019	e2_a46_rp	0.9838313	1.26E+04	0	0	3.04300104	0	0
4/6/2019	e2_a47	2.21137802	2.48E+04	0.40905337	0.23883968	0.80194568	0	0
4/6/2019	e2_a47_rp	2.4500215	6.88E+03	0.44168475	0	3.00398377	0	0
4/6/2019	e2_a48	2.11565372	1.20E+04	0	0	1.2979981	0	0
4/6/2019	e2_a48_rp	0.747192	1.51E+04	0	0	2.32046496	0	0
5/18/2019	e2_a49	0.9838313	2.59E+04	0	0	1.70775314	0	0

5/18/2019	e2_a49_rp	1.99541006	2.21E+04	0.44317675	0	1.36017527	0	0
11/4/2018	e2_a5	1.4998891	1.92E+04	0	0.2267481	1.57430514	0	0
11/4/2018	e2_a5_rp	1.20693618	1.98E+04	0	0	1.36017527	0	0.40771782
11/4/2018	e2_a6	1.4998891	2.27E+04	0	0	1.57430514	0	0.40158085
11/4/2018	e2_a6_rp	0.64621336	1.87E+04	0	0	2.54547406	0	0
11/4/2018	e2_a7	1.69347841	2.53E+04	0.40905337	0	1.57430514	0	0
11/4/2018	e2_a7_rp	1.4998891	1.37E+04	0.35240268	0.24006977	2.60957148	0	0
12/8/2018	e2_a8	2.11565372	2.30E+03	0	0	2.72554326	0.87916642	0
12/8/2018	e2_a8_rp	2.26559442	3.37E+03	0.42727093	0	2.32046496	0.87368077	0
12/8/2018	e2_a9	0.38909282	1.24E+04	0	0	2.40182065	0	0
12/8/2018	e2_a9_rp	1.99541006	1.90E+04	0	0	1.36017527	0.84860483	0
1/5/2019	e2_b1	1.37116405	3.79E+03	0.4457337	0	3.41243488	0	0
1/5/2019	e2_b1_rp	0.64621336	7.83E+03	0.35240268	0	2.23112597	0.87169061	0
1/5/2019	e2_b2	0.64621336	2.21E+04	0	0.24013474	0	0	0
1/5/2019	e2_b2_rp	0	2.85E+04	0	0	0.80194568	0	0
4/6/2019	e2_b3	0.9838313	2.34E+04	0.35240268	0	1.89470902	0	0.39574762
4/6/2019	e2_b3_rp	2.62300306	2.09E+04	0	0	1.89470902	0.7908802	0
4/6/2019	e2_b4	2.69176869	1.92E+03	0	0	1.96004126	0.86203403	0
4/6/2019	e2_b4_rp	1.7695065	2.46E+03	0.42727093	0	2.54547406	0	0
5/5/2019	e2_b5	2.11565372	5.73E+03	0	0	3.57303168	0	0
5/5/2019	e2_b5_rp	1.97211785	1.28E+04	0	0.24014011	0	0	0
5/18/2019	e2_b6	1.83597982	1.36E+04	0	0	2.76545249	0	0
5/18/2019	e2_b6_rp	1.89488946	1.07E+04	0.35240268	0	2.32046496	0.85158808	0
6/8/2019	e2_b7	1.99541006	2.04E+04	0.35240268	0.2267481	0.68657594	0	0.3816041
6/8/2019	e2_b7_rp	1.7695065	1.76E+04	0	0	2.13209312	0	0
6/8/2019	e2_b8	0.52874921	2.09E+04	0	0.2267481	1.74828819	0	0
6/8/2019	e2_b8_rp	0.64621336	2.54E+04	0	0	1.89470902	0	0
Lambda Value =		-0.204722783	2.426402932	-2.234798987	-4.164195276	-0.027528604	-1.12193801	-2.441191125

Table 5.3 Transformed data output for e3. The abbreviation for coarse woody debris is CWD.

Date	ID	Microstory	Leaflitter	Moss	Woody brush	CWD	Logs	Rocks
10/28/2018	e3_a1	1.55229046	1338.278898	0	0	1.03681836	1.2730114	0
10/28/2018	e3_a1_rp	2.26563872	1338.278898	0	0	0	0	0.31550916
10/28/2018	e3_a2	1.55229046	1338.278898	0	0	1.03681836	1.2730114	0
10/28/2018	e3_a2_rp	2.62495674	5.90116713	0.68572052	0	0	1.44810966	0.36914381
10/28/2018	e3_a3	2.33486227	948.0938002	0	0	2.35274707	0	0
10/28/2018	e3_a3_rp	3.15960012	12.59483915	0	0.50069901	0	0	0
10/28/2018	e3_a4	2.30137029	900.4613796	0.59718968	0	2.35274707	0	0
10/28/2018	e3_a4_rp	1.66571829	1629.788435	0.43719484	0	0	0	0
11/3/2018	e3_a5	2.70901686	657.5906087	0	0	0	1.2730114	0
11/3/2018	e3_a5_rp	2.60624628	657.5906087	0.64851988	0	0	1.2730114	0
11/3/2018	e3_a6	2.36636234	1097.25464	0	0	1.86541884	0	0
11/3/2018	e3_a6_rp	2.50035327	996.7750585	0.43719484	0	0	0	0.37110045
11/3/2018	e3_a7	2.36636234	900.4613796	0	0	1.63128423	1.2730114	0
11/3/2018	e3_a7_rp	2.73890669	830.9962428	0	0	0	0	0
11/3/2018	e3_a8	2.70901686	364.5271422	0.43719484	0	1.63128423	1.40065978	0
11/3/2018	e3_a8_rp	2.30137029	1338.278898	0	0	0	0	0
11/3/2018	e3_a9	2.50035327	637.145356	0	0	0	1.4149734	0
11/3/2018	e3_a9_rp	2.78046786	657.5906087	0.63824469	0	0	0	0
11/3/2018	e3_a10	2.52340112	763.9356288	0	0	0	1.35291807	0
11/3/2018	e3_a10_rp	1.84459639	1599.533903	0	0	0	0	0
11/3/2018	e3_a11	2.36636234	972.303795	0	0	0	1.31085756	0
11/3/2018	e3_a11_rp	1.66571829	720.5785915	0.64851988	0	0	0	0
11/3/2018	e3_a12	2.70901686	657.5906087	0	0	0	1.2730114	0
11/3/2018	e3_a12_rp	2.22737212	89.59849316	0.68119887	0.503595	0	1.45682215	0
11/3/2018	e3_a13	2.54543937	786.0202501	0.63824469	0	0	1.22225139	0
11/3/2018	e3_a13_rp	2.62495674	996.7750585	0	0	0	0	0
11/3/2018	e3_a14	2.56654726	900.4613796	0	0	0	1.1894918	0
11/3/2018	e3_a14_rp	2.66035409	786.0202501	0	0	0	1.1894918	0
11/3/2018	e3_a15	2.56654726	900.4613796	0	0	0	1.1894918	0
11/3/2018	e3_a15_rp	2.60624628	1021.506671	0	0	0	0	0
11/3/2018	e3_a16	2.56654726	900.4613796	0	0	0	1.1894918	0
11/3/2018	e3_a16_rp	2.70901686	742.1213714	0	0	0	0	0.37215278
11/3/2018	e3_a17	2.50035327	1149.038865	0	0	0	0	0
11/3/2018	e3_a17_rp	2.9895313	380.662434	0	0	0	0	0
11/24/2018	e3_a18	1.55229046	380.662434	0.66824089	0	1.47914453	1.49237906	0
11/24/2028	e3_a18_rp	1.41437557	830.9962428	0.6650843	0	2.30083927	0	0.3737283
11/24/2028	e3_a19	1.23986601	742.1213714	0.63824469	0	2.60050608	0	0.3738934
11/24/2028	e3_a19_rp	1.23986601	1255.662666	0	0	2.48809895	0	0
11/24/2028	e3_a20	1.23986601	1366.318017	0	0	2.30083927	0	0
11/24/2028	e3_a20_rp	1.00524158	1510.233632	0	0	1.86541884	0	0.35434996
11/24/2028	e3_a21	1.55229046	448.1704102	0.59718968	0	1.95922926	1.48978759	0
11/24/2028	e3_a21_rp	1.76168037	972.303795	0	0	2.69639804	0	0.31550916
11/24/2028	e3_a22	1.00524158	1123.018762	0.54937996	0	1.03681836	1.39265588	0
11/24/2028	e3_a22_rp	1.91742093	1394.60609	0	0	1.75763332	0	0

11/24/2028	e3_a23	1.55229046	1480.956865	0	0	1.86541884	0	0
11/24/2028	e3_a23_rp	1.23986601	1451.926222	0	0	2.1163734	0	0
11/24/2028	e3_a24	1.55229046	1480.956865	0	0	1.86541884	0	0
11/24/2028	e3_a24_rp	2.45085861	1201.843703	0	0	0	0	0
12/13/2018	e3_a25	1.00524158	1569.522821	0	0	0.66819801	0	0.37215278
12/13/2018	e3_a25_rp	0.65516546	1366.318017	0	0	0	1.2730114	0.37110045
12/13/2018	e3_a26	0.39226537	1296.68862	0.54937996	0	1.75763332	1.2730114	0
12/13/2018	e3_a26_rp	0.65516546	1706.485632	0	0	1.38987026	0	0
12/13/2018	e3_a27	1.00524158	1645.006792	0.50695971	0	0	0	0.36500701
12/13/2018	e3_a27_rp	0.65516546	1698.747907	0.19063641	0.47937119	0	0	0
12/13/2018	e3_a28	0.65516546	1510.233632	0	0	2.1163734	0	0
12/13/2018	e3_a28_rp	1.23986601	1722.006302	0	0.37703687	0	0	0
12/13/2018	e3_a29	0.21910596	1532.352317	0.59718968	0.49436029	0	0	0.31550916
12/13/2018	e3_a29_rp	0	1387.510772	0.19063641	0	2.40095975	0	0
12/13/2018	e3_a30	0	1310.489469	0	0	1.28887789	1.35291807	0
12/13/2018	e3_a30_rp	1.00524158	1660.28577	0	0	1.47914453	0	0
12/13/2018	e3_a31	0	1310.489469	0	0	1.28887789	1.35291807	0
12/13/2018	e3_a31_rp	1.00524158	1423.142396	0	0	2.24465684	0	0
12/13/2018	e3_a32	0	1310.489469	0	0	1.28887789	1.35291807	0
12/13/2018	e3_a32_rp	0.21910596	1824.355303	0	0	0.39684125	0	0
12/13/2018	e3_a33	0	1310.489469	0	0	1.28887789	1.35291807	0
12/13/2018	e3_a33_rp	1.23986601	1592.008284	0	0	1.66494588	0	0
12/29/2019	e3_a34	1.55229046	1310.489469	0	0	2.30083927	0	0
12/29/2019	e3_a34_rp	0	1123.018762	0	0	2.75322868	0	0
12/29/2019	e3_a35	1.55229046	1310.489469	0	0	2.30083927	0	0
12/29/2019	e3_a35_rp	1.41437557	1149.038865	0	0	1.95922926	0	0.37382246
12/29/2019	e3_a36	0	1310.489469	0	0	2.52773507	0	0
12/29/2019	e3_a36_rp	0	1848.333472	0	0	0	0	0
12/29/2019	e3_a37	1.00524158	1123.018762	0	0	2.63406796	0	0.35434996
12/29/2019	e3_a37_rp	0	1175.314118	0	0	2.69639804	0	0
12/29/2019	e3_a38	1.66571829	1071.747342	0	0	2.63406796	0	0
12/29/2019	e3_a38_rp	1.55229046	678.3120363	0	0	3.05090937	0	0
1/19/2019	e3_a39	0	1691.025268	0	0	1.63128423	0	0
1/19/2019	e3_a39_rp	2.62495674	413.8265487	0	0.50069901	2.52773507	0	0
1/19/2019	e3_a40	0.21910596	1745.40021	0	0	1.28887789	0	0
1/19/2019	e3_a40_rp	0.65516546	1480.956865	0	0	1.75763332	1.09906172	0
1/19/2019	e3_a41	0	3.33954765	0.68855729	0	0	1.1894918	0
1/19/2019	e3_a41_rp	0	0	0.68826912	0	2.72544231	0	0
1/19/2019	e3_a42	0	3.33954765	0.68855729	0	0	1.1894918	0
1/19/2019	e3_a42_rp	0	763.9356288	0	0	3.06756247	0	0
1/26/2019	e3_a43	0	1539.755842	0	0	2.1163734	0	0
1/26/2019	e3_a43_rp	1.66571829	808.3741445	0	0.50193261	2.60050608	0	0
1/26/2019	e3_a44	1.66571829	720.5785915	0	0.49436029	1.75763332	1.37455338	0.37277235
1/26/2019	e3_a44_rp	1.41437557	972.303795	0.63824469	0.48421159	0	0	0.37407407
1/26/2019	e3_a45	1.23986601	877.0408785	0	0.49856217	2.40095975	1.2496617	0

1/26/2019	e3_a45_rp	0.65516546	1201.843703	0	0.50193261	2.04215489	0	0
1/26/2019	e3_a46	1.23986601	678.3120363	0.54937996	0.50433915	1.28887789	0	0.3736003
1/26/2019	e3_a46_rp	1.00524158	465.7805715	0	0.50487723	1.03681836	0	0
1/26/2019	e3_a47	0	333.1592837	0.66104757	0.50236206	2.77985697	1.36424448	0
1/26/2019	e3_a47_rp	1.23986601	1660.28577	0	0	1.03681836	0	0.31550916
1/26/2019	e3_a48	0	699.3084261	0.54937996	0.50396898	0	1.40065978	0
1/26/2019	e3_a48_rp	1.76168037	996.7750585	0.54937996	0.49685053	2.35274707	0	0
1/26/2019	e3_a49	0	699.3084261	0.54937996	0.50396898	0	1.40065978	0
1/26/2019	e3_a49_rp	0.65516546	924.1460106	0	0.50451631	1.03681836	0	0
2/9/2019	e3_a50	0.21910596	1539.755842	0	0.18037453	0.39684125	1.2496617	0
2/9/2019	e3_a50_rp	0.85070595	1451.926222	0.19063641	0	2.15073161	0	0.29033566
3/12/2019	e3_a51	0.85070595	1722.006302	0	0.18037453	0.66819801	0	0.33136183
3/12/2019	e3_a51_rp	0.65516546	1698.747907	0	0	0.9590487	0	0.35434996
3/12/2019	e3_a52	0.39226537	906.3578134	0	0	1.34101821	1.45682215	0
3/12/2019	e3_a52_rp	1.41437557	1488.253009	0.60496215	0.18037453	1.34101821	0	0.31550916
3/12/2019	e3_a53	0.39226537	906.3578134	0	0	1.34101821	1.45682215	0
3/12/2019	e3_a53_rp	1.28791174	1607.074738	0.43719484	0.18037453	1.23300047	0	0.24757901
3/12/2019	e3_a54	0.39226537	906.3578134	0	0	1.34101821	1.45682215	0
3/12/2019	e3_a54_rp	0.65516546	1554.608777	0.19063641	0	1.47914453	0	0.36976398
3/31/2019	e3_b1	0.65516546	1569.522821	0.59718968	0.37703687	1.03681836	0	0.35434996
3/31/2019	e3_b1_rp	0.39226537	1614.630779	0.59718968	0	1.03681836	0	0.35434996
3/31/2019	e3_a55	1.00524158	1423.142396	0.43719484	0.37703687	1.47914453	1.14944868	0
3/31/2019	e3_a55_rp	1.00524158	1310.489469	0.43719484	0.37703687	1.47914453	1.2730114	0
3/31/2019	e3_a56	1.23986601	1228.626816	0.43719484	0	1.03681836	1.35291807	0
3/31/2019	e3_a56_rp	1.23986601	1366.318017	0.43719484	0	1.86541884	1.09906172	0
3/31/2019	e3_a57	1.23986601	1228.626816	0.43719484	0	1.03681836	1.35291807	0
3/31/2019	e3_a57_rp	1.00524158	1722.006302	0	0.37703687	0.66819801	0	0
3/31/2019	e3_a58	1.00524158	1324.352926	0.3065521	0.37703687	1.03681836	0.94203624	0
3/31/2019	e3_a58_rp	1.41437557	1569.522821	0	0.47261942	1.03681836	0	0
4/27/2019	e3_a59	1.91742093	1149.038865	0	0	1.63128423	1.2730114	0
4/27/2019	e3_a59_rp	2.30137029	1201.843703	0	0.37703687	1.47914453	0	0
4/27/2019	e3_a60	2.4762063	520.3450262	0	0.44770565	1.95922926	1.39265588	0
4/27/2019	e3_a60_rp	2.33486227	1046.497728	0	0	2.1163734	0	0
Lambda Value =		-0.164161324	1.751360919	-1.450250995	-1.979886434	-0.106426298	-0.598529515	-2.672244317

Table 5.4 Transformed data output for the composite of all elevations. The abbreviation for coarse woody debris is CWD.

Date	ID	Microstory	Leaflitter	Moss	Woody brush	CWD	Logs	Rocks
11/10/2018	e1_a1	0.96264175	9.84E+00	0.67192861	0.37997441	1.88001247	0.92172052	0.42517108
11/10/2018	e1_a1_rp	1.44895111	1.17E+04	0.19355952	0	1.88001247	0	0.3634649
11/10/2018	e1_b1	1.58866522	1.17E+04	0.45594983	0	1.73578758	0	0
11/10/2018	e1_b1_rp	1.29422369	8.35E+03	0.67192861	0	0.68466155	1.00060987	0
11/10/2018	e1_a2	0.73514653	1.47E+04	0	0	1.07739731	0	0
11/10/2018	e1_a2_rp	1.69726049	9.51E+03	0.19355952	0	1.22522688	0.95668232	0
11/10/2018	e1_a3	1.44895111	1.39E+04	0	0	0.40255159	0	0
11/10/2018	e1_a3_rp	0.73514653	1.22E+04	0.69174071	0	0.90150119	0	0.41095643
11/23/2018	e1_a4	0.52279507	1.34E+04	0	0	1.94430683	0	0
11/23/2018	e1_a4_rp	1.25712866	1.16E+04	0.45594983	0	1.41027018	0.84676821	0.34310436
11/23/2018	e1_a6	0.96264175	1.14E+04	0.65813419	0	1.56418052	0	0.41775592
11/23/2018	e1_a6_rp	1.62766422	2.04E+03	0.7410522	0.36169067	3.00479699	0.99610027	0
11/23/2018	e1_b2	2.2410179	7.80E+03	0	0.32061154	0.68466155	0	0
11/23/2018	e1_b2_rp	0.63725803	1.15E+04	0.45594983	0	0.79933189	0.96182919	0
11/23/2018	e1_b3	0.52279507	1.55E+04	0	0	0.22225921	0	0
11/23/2018	e1_b3_rp	0.63725803	1.43E+04	0.58320933	0	0.79933189	0	0
12/7/2018	e1_a7	1.17458973	1.06E+04	0.58320933	0	1.77405815	0.90104432	0
12/7/2018	e1_a7_rp	0.63725803	1.16E+04	0.39696776	0	0.79933189	0.96182919	0
12/7/2018	e1_a8	0.52279507	1.55E+04	0	0	0.22225921	0	0
12/7/2018	e1_a8_rp	0.89552501	1.50E+04	0	0	0.40255159	0	0
12/7/2018	e1_a9	0.63725803	1.43E+04	0.61644345	0	0.22225921	0	0.26195757
12/7/2018	e1_a9_rp	0.73514653	1.44E+04	0.50008636	0	0.22225921	0	0.3634649
12/7/2018	e1_a10	0.73514653	1.42E+04	0.19355952	0	1.41027018	0	0
12/7/2018	e1_a10_rp	0.63725803	1.28E+04	0.19355952	0	0.55407593	0.92172052	0
12/7/2018	e1_a11	2.09475035	8.79E+03	0	0	1.73578758	0	0
12/7/2018	e1_a11_rp	0.63725803	1.27E+04	0.58320933	0	0.22225921	0	0.42316266
12/14/2018	e1_a10.1	0.96264175	1.04E+04	0.72203275	0	1.56418052	0	0
12/14/2018	e1_a10.1_rp	0.217128	9.24E+03	0.7148183	0.37778966	1.73578758	0.87376449	0
12/14/2018	e1_a11.1	0.8203389	1.43E+04	0	0	1.3526283	0	0
12/14/2018	e1_a11.1_rp	1.21737242	1.09E+04	0.31476588	0	0.40255159	0	0.42640081
12/14/2018	e1_a12.1	0.96264175	9.58E+03	0.72760982	0	1.73578758	0.83604024	0
12/14/2018	e1_a12.1_rp	0.217128	1.49E+04	0	0	1.22522688	0	0
12/21/2018	e1_b4	0.63725803	1.55E+04	0	0	0	0	0
12/21/2018	e1_b4_rp	0.38589458	1.44E+04	0	0	1.46450251	0	0
12/21/2018	e1_a13	1.81128557	1.16E+04	0	0	1.3526283	0	0
12/21/2018	e1_a13_rp	0.217128	1.19E+04	0.61644345	0.37997441	1.3526283	0	0.34310436
12/30/2018	e1_a14	1.36160124	1.40E+04	0	0	0.68466155	0	0
12/30/2018	e1_a14_rp	0.52279507	1.08E+04	0	0	2.64009582	0	0
12/30/2018	e1_a15	0.8203389	5.71E+03	0.74495008	0	1.3526283	0	0.42718588
12/30/2018	e1_a15_rp	0.217128	8.22E+03	0.74786687	0	1.73578758	0	0.41095643
12/30/2018	e1_a16	0.96264175	1.50E+04	0	0	0.22225921	0	0
12/30/2018	e1_a16_rp	0.217128	1.29E+04	0.65813419	0	1.73578758	0	0
12/30/2018	e1_a17	0.52279507	1.32E+04	0.45594983	0	1.88001247	0	0
12/30/2018	e1_a17_rp	0.63725803	1.34E+04	0.67192861	0	1.15425908	0	0

1/25/2019	e1_a18	0.52279507	1.19E+04	0	0	0.68466155	0.96182919	0
1/25/2019	e1_a18_rp	0.63725803	1.33E+04	0	0	1.3526283	0	0.41498291
2/2/2019	e1_a19	0.96264175	1.30E+04	0.19355952	0.25029008	1.3526283	0.33797047	0.3949089
2/2/2019	e1_a19_rp	1.17458973	1.08E+04	0.65813419	0	1.56418052	0.87376449	0
2/2/2019	e1_a20	1.3289623	1.01E+04	0.64028984	0.37997441	1.88001247	0	0
2/2/2019	e1_a20_rp	1.3289623	1.08E+04	0.31476588	0.37997441	1.3526283	0	0.41095643
2/2/2019	e1_a21	1.07807533	1.36E+04	0	0	1.56418052	0	0
2/2/2019	e1_a21_rp	1.17458973	7.56E+03	0.74315093	0	1.07739731	0.83604024	0.42120126
2/2/2019	e1_a22	1.17458973	9.85E+03	0.64028984	0.37778966	1.07739731	0.92172052	0
2/2/2019	e1_a22_rp	0.63725803	1.03E+04	0.58320933	0.25029008	1.07739731	0.97858492	0
3/1/2019	e1_a18.1	0.96264175	4.90E+00	0.64028984	0	1.3526283	0	0
3/1/2019	e1_a18.1_rp	0.96264175	8.66E+03	0.72499051	0.1691856	0.55407593	0	0.42661959
3/1/2019	e1_a18.2	0.73514653	1.42E+04	0.19355952	0.33725658	0.90150119	0	0.26195757
3/1/2019	e1_a18.2_rp	1.21737242	1.13E+04	0.39696776	0	0.68466155	0.9448273	0.17386117
3/23/2019	e1_a25	1.77179972	1.10E+04	0	0	1.81077515	0	0
3/23/2019	e1_a25_rp	1.62766422	1.06E+04	0.67192861	0.32061154	1.15425908	0	0.3949089
3/23/2019	e1_a26	1.3289623	1.34E+04	0	0.32061154	1.07739731	0	0
3/23/2019	e1_a26_rp	1.44895111	1.16E+04	0.67192861	0	0.68466155	0	0.41095643
3/23/2019	e1_a27	1.17458973	9.31E+03	0.45594983	0.37778966	1.73578758	0.93795033	0
3/23/2019	e1_a27_rp	1.44895111	1.16E+04	0.67192861	0	0.68466155	0	0.41095643
3/23/2019	e1_b7	1.69726049	1.22E+04	0	0.32061154	1.07739731	0	0
3/23/2019	e1_b7_rp	1.17458973	1.16E+04	0.67192861	0.32061154	1.07739731	0	0.41095643
3/23/2019	e1_a28	1.3289623	1.31E+04	0.45594983	0.32061154	1.07739731	0	0
3/23/2019	e1_a28_rp	1.54628393	9.58E+03	0.64028984	0.37997441	1.56418052	0	0.3949089
3/23/2019	e1_b8	1.62766422	6.65E+03	0.58320933	0.32061154	1.07739731	1.01448693	0
3/23/2019	e1_b8_rp	1.17458973	5.81E+03	0.72203275	0.36169067	1.73578758	1.00060987	0.3949089
3/29/2019	e1_a29	1.3289623	5.03E+03	0.45594983	0.37323225	2.29835828	1.01448693	0.3949089
3/29/2019	e1_a29_rp	1.07807533	1.27E+04	0.39696776	0.32061154	1.3526283	0	0.3949089
3/29/2019	e1_a30	1.42142162	1.33E+04	0	0.1691856	1.22522688	0	0
3/29/2019	e1_a30_rp	1.17458973	8.35E+03	0.19355952	0.1691856	2.39698964	0.96182919	0
4/7/2019	e1_a31	1.72853878	1.08E+04	0.39696776	0	1.6540286	0	0.3949089
4/7/2019	e1_a31_rp	1.44895111	8.79E+03	0.64028984	0	1.73578758	0.96182919	0
4/7/2019	e1_b9	1.17458973	1.38E+04	0.45594983	0.32061154	0.68466155	0	0
4/7/2019	e1_b9_rp	1.44895111	1.16E+04	0.45594983	0	2.00430734	0	0
11/4/2018	e2_a1	0.96264175	1.31E+04	0	0.36169067	1.56418052	0	0
11/4/2018	e2_a1_rp	2.63021721	6.03E+02	0	0.36169067	2.00430734	0	0
11/4/2018	e2_a2	2.45328259	3.38E+03	0.39696776	0.36169067	1.3526283	0	0.3949089
11/4/2018	e2_a2_rp	1.72853878	7.21E+03	0	0	2.92697661	0	0
11/4/2018	e2_a3	0.38589458	1.03E+04	0	0	1.3526283	0.99101267	0
11/4/2018	e2_a3_rp	1.17458973	1.02E+04	0.53420573	0	0.79933189	0.96182919	0.3949089
11/4/2018	e2_a4	2.06837671	4.31E+03	0.45594983	0	1.3526283	0	0.42742907
11/4/2018	e2_a4_rp	0.52279507	9.78E+03	0	0	2.16340308	0.96182919	0
11/4/2018	e2_a5	0	1.19E+04	0	0	2.45128272	0	0
11/4/2018	e2_a5_rp	0.52279507	9.78E+03	0	0	2.16340308	0.96182919	0
11/4/2018	e2_a6	0.96264175	9.05E+03	0	0	2.1134536	0.97858492	0

11/4/2018	e2_a6_rp	0.52279507	9.78E+03	0	0	2.16340308	0.96182919	0
11/4/2018	e2_a7	1.39235872	1.33E+04	0	0	1.3526283	0	0
11/4/2018	e2_a7_rp	2.09475035	5.81E+03	0	0	1.88001247	0.78028918	0.42571947
12/8/2018	e2_a8	1.54628393	5.03E+03	0.58320933	0	3.17321906	0	0.41775592
12/8/2018	e2_a8_rp	1.3289623	1.93E+03	0	0	3.78050476	0	0
12/8/2018	e2_a9	0.96264175	8.79E+03	0	0.38231705	2.45128272	0	0.34310436
12/8/2018	e2_a9_rp	1.69726049	7.56E+03	0	0	2.88527146	0	0
12/8/2018	e2_a10	2.52686931	8.56E+02	0	0	2.79531216	0	0.41775592
12/8/2018	e2_a10_rp	1.90200737	1.13E+04	0	0	1.07739731	0	0
12/8/2018	e2_a11	0.63725803	2.92E+03	0	0	1.3526283	1.04992012	0
12/8/2018	e2_a11_rp	1.62766422	8.92E+03	0.64028984	0	1.6540286	0.93795033	0
12/16/2018	e2_a12	1.3289623	8.79E+03	0	0	1.88001247	0.98522651	0
12/16/2018	e2_a12_rp	1.54628393	6.87E+03	0	0	2.45128272	0.98522651	0
12/16/2018	e2_a13	2.0096936	7.10E+03	0	0.38328614	0	0	0
12/16/2018	e2_a13_rp	1.75783013	6.01E+03	0.45594983	0	2.29835828	0.99610027	0
12/16/2018	e2_a14	1.90200737	9.58E+03	0	0	2.1134536	0	0
12/16/2018	e2_a14_rp	1.69726049	9.05E+03	0	0.37323225	1.07739731	0.9510404	0
12/16/2018	e2_a15	1.62766422	7.56E+03	0.45594983	0.38116252	2.58155836	0	0
12/16/2018	e2_a15_rp	1.62766422	8.04E+03	0	0.37778966	2.64009582	0	0
12/16/2018	e2_a16	0.96264175	1.41E+04	0	0	1.3526283	0	0
12/16/2018	e2_a16_rp	1.44895111	3.35E+03	0	0	3.57908301	0	0
12/16/2018	e2_a17	1.69726049	1.07E+04	0	0	1.88001247	0	0.3949089
12/16/2018	e2_a17_rp	1.54628393	7.10E+03	0	0	2.64009582	0.9510404	0
12/16/2018	e2_a18	1.75783013	6.43E+03	0	0	2.58155836	0.96182919	0
12/16/2018	e2_a18_rp	1.44895111	1.07E+04	0	0	1.3526283	0	0.42517108
12/16/2018	e2_a19	1.90200737	2.78E+03	0	0	2.00430734	1.03970593	0
12/16/2018	e2_a19_rp	1.44895111	1.07E+04	0	0	1.3526283	0	0.42517108
12/16/2018	e2_a20	2.09475035	7.33E+03	0	0	2.37812365	0	0
12/16/2018	e2_a20_rp	1.44895111	1.07E+04	0	0	1.3526283	0	0.42517108
12/22/2018	e2_a21	1.44895111	1.01E+04	0	0	2.51883176	0	0
12/22/2018	e2_a21_rp	2.0096936	2.04E+03	0.64028984	0	2.29835828	1.03643756	0
12/22/2018	e2_a22	1.90200737	7.33E+03	0	0	2.74658066	0	0
12/22/2018	e2_a22_rp	0.52279507	1.41E+04	0.19355952	0	0.68466155	0	0.41095643
12/22/2018	e2_a23	1.3289623	1.32E+04	0	0	1.5157004	0	0
12/22/2018	e2_a23_rp	1.62766422	1.61E+03	0.74906269	0.37323225	2.64009582	1.01719371	0
12/22/2018	e2_a24	1.3289623	4.48E+03	0.45594983	0	2.21070106	1.03254151	0
12/22/2018	e2_a24_rp	0.63725803	1.50E+04	0	0	0.79933189	0	0
12/22/2018	e2_a25	0.38589458	1.42E+04	0	0	1.61021268	0	0
12/22/2018	e2_a25_rp	0.217128	1.10E+04	0	0	1.46450251	0.97087985	0
1/5/2019	e2_b1	0.38589458	1.43E+04	0	0	1.56418052	0	0
1/5/2019	e2_b1_rp	0.96264175	1.13E+04	0	0	1.88001247	0.90104432	0
1/5/2019	e2_b2	1.44895111	9.31E+03	0.45594983	0	2.64009582	0	0
1/5/2019	e2_b2_rp	0.96264175	1.13E+04	0	0	1.88001247	0.90104432	0
1/5/2019	e2_a26	2.51196318	1.52E+03	0.64028984	0	2.51883176	0	0
1/5/2019	e2_a26_rp	2.09475035	3.97E+03	0.70517723	0	2.96676307	0	0

1/5/2019	e2_a27	2.0096936	8.29E+03	0	0	2.29835828	0	0
1/5/2019	e2_a27_rp	0.96264175	1.19E+04	0.7148183	0	1.3526283	0	0
1/5/2019	e2_a28	0.52279507	1.35E+04	0	0	1.88001247	0	0
1/5/2019	e2_a28_rp	1.69726049	3.35E+03	0	0	3.5201676	0	0
1/5/2019	e2_a29	2.47120046	1.61E+03	0	0	2.88527146	0	0
1/5/2019	e2_a29_rp	1.17458973	1.22E+04	0	0	1.56418052	0	0.41775592
1/5/2019	e2_a30	0.96264175	1.34E+04	0	0	1.73578758	0	0
1/5/2019	e2_a30_rp	1.17458973	1.22E+04	0	0	1.56418052	0	0.41775592
1/21/2019	e2_a31	0.63725803	1.34E+04	0.58320933	0	1.56418052	0	0
1/21/2019	e2_a31_rp	1.44895111	1.42E+03	0	0	2.69496088	1.04761435	0
1/21/2019	e2_a32	2.14265409	6.87E+03	0	0	2.37812365	0	0
1/21/2019	e2_a32_rp	1.90200737	2.27E+03	0.73561983	0	3.36426953	0	0
1/21/2019	e2_a33	2.43429494	4.14E+03	0	0	1.73578758	0	0
1/21/2019	e2_a33_rp	1.90200737	7.10E+03	0	0	2.79531216	0	0
1/21/2019	e2_a34	1.94107428	6.01E+03	0	0	2.96676307	0	0
1/21/2019	e2_a34_rp	2.0096936	5.22E+03	0	0	1.56418052	1.01448693	0
1/21/2019	e2_a35	1.81128557	6.65E+03	0	0	2.96676307	0	0
1/21/2019	e2_a35_rp	1.54628393	1.42E+03	0.73203442	0	3.36426953	0	0.42702841
1/27/2019	e2_a36	0	1.24E+03	0	0	3.63414665	1.01448693	0
1/27/2019	e2_a36_rp	0.63725803	1.31E+04	0.58320933	0	1.3526283	0	0.3949089
1/27/2019	e2_a37	0.73514653	1.40E+04	0	0	1.56418052	0	0
1/27/2019	e2_a37_rp	0.63725803	1.31E+04	0.58320933	0	1.3526283	0	0.3949089
1/27/2019	e2_a38	0.63725803	1.22E+04	0	0	2.29835828	0	0
1/27/2019	e2_a38_rp	1.12833818	7.74E+03	0.61644345	0	1.07739731	1.01448693	0
1/27/2019	e2_a39	0.63725803	1.11E+04	0	0	1.46450251	0.96182919	0
1/27/2019	e2_a39_rp	0.52279507	1.46E+04	0.19355952	0	1.07739731	0	0.26195757
1/27/2019	e2_a40	0.8203389	1.03E+04	0.45594983	0	1.56418052	0.97087985	0
1/27/2019	e2_a40_rp	0.217128	1.47E+04	0.58320933	0	0	0	0.34310436
1/27/2019	e2_a41	0.63725803	1.19E+04	0	0.38297524	0	0	0
1/27/2019	e2_a41_rp	0	1.25E+04	0.45594983	0	1.88001247	0	0.41095643
2/24/2019	e2_a42	0.63725803	1.16E+04	0	0	2.45128272	0	0
2/24/2019	e2_a42_rp	1.60855668	1.08E+04	0.45594983	0	1.84605788	0	0.40050285
2/24/2019	e2_a43	0.73514653	1.04E+04	0.45594983	0	2.62582422	0	0
2/24/2019	e2_a43_rp	1.60855668	1.08E+04	0.45594983	0	1.84605788	0	0.40050285
2/24/2019	e2_a44	0.38589458	1.32E+04	0.19355952	0.37778966	1.3526283	0	0
2/24/2019	e2_a44_rp	0	6.65E+03	0.58320933	0	3.10975518	0	0.41775592
3/24/2019	e2_a45	0.8203389	1.47E+04	0	0	0.99359488	0	0
3/24/2019	e2_a45_rp	1.47508712	9.78E+03	0.45594983	0.1691856	2.25561078	0	0.41316701
3/24/2019	e2_a46	1.3289623	1.38E+04	0	0.1691856	0.90150119	0	0
3/24/2019	e2_a46_rp	0.63725803	1.28E+04	0	0	2.1134536	0	0
3/24/2019	e2_a46.1	0.52279507	7.92E+03	0.67192861	0	2.43355374	0.96182919	0
3/24/2019	e2_a46.1_rp	0.63725803	1.28E+04	0	0	2.1134536	0	0
4/6/2019	e2_b3	0.96264175	1.02E+04	0.31476588	0.32061154	1.41027018	0.96182919	0.34310436
4/6/2019	e2_b3_rp	0.38589458	1.16E+04	0	0	2.48570512	0	0
4/6/2019	e2_b4	1.17458973	1.38E+04	0	0.1691856	1.29112817	0	0

4/6/2019	e2_b4_rp	0.38589458	1.16E+04	0	0	2.48570512	0	0
4/6/2019	e2_a47	1.07807533	1.31E+04	0	0	1.81077515	0	0
4/6/2019	e2_a47_rp	1.62766422	1.13E+04	0	0	2.00430734	0	0
4/6/2019	e2_a48	0.8203389	1.41E+04	0	0.29439665	1.22522688	0.2015742	0
4/6/2019	e2_a48_rp	0.8203389	1.33E+04	0	0	1.88001247	0	0
5/5/2019	e2_b5	0.96264175	1.32E+04	0.58320933	0.3689297	0.79933189	0	0
5/5/2019	e2_b5_rp	1.66373829	6.98E+03	0	0	3.00479699	0	0
5/18/2019	e2_b6	2.45328259	1.20E+03	0	0	1.94430683	1.01448693	0
5/18/2019	e2_b6_rp	1.69726049	3.35E+03	0	0	3.5201676	0	0
5/18/2019	e2_a49	2.3040909	6.71E+03	0	0	1.29112817	0	0
5/18/2019	e2_a49_rp	0.73514653	1.38E+04	0	0	1.69582871	0	0
6/8/2019	e2_b7	1.8810416	7.50E+03	0	0	2.73395939	0	0
6/8/2019	e2_b7_rp	1.81128557	1.10E+04	0.45594983	0.32061154	0.68466155	0	0.3949089
6/8/2019	e2_b8	1.90200737	1.04E+04	0	0.32061154	1.56418052	0	0
6/8/2019	e2_b8_rp	1.69726049	1.13E+04	0	0.32061154	1.73578758	0	0
10/28/2018	e3_a1	0.63725803	1.33E+04	0.45594983	0.34837931	0.68466155	0.68910193	0.34310436
10/28/2018	e3_a1_rp	1.44895111	1.04E+04	0	0	1.07739731	0.96182919	0
10/28/2018	e3_a2	2.04011101	1.04E+04	0	0	0	0	0.34310436
10/28/2018	e3_a2_rp	1.44895111	1.04E+04	0	0	1.07739731	0.96182919	0
10/28/2018	e3_a3	2.31823322	9.84E+00	0.75831158	0	0	1.03107057	0.41775592
10/28/2018	e3_a3_rp	2.09475035	6.65E+03	0	0	2.58155836	0	0
10/28/2018	e3_a4	2.70584947	2.54E+01	0	0.3828252	0	0	0
10/28/2018	e3_a4_rp	2.06837671	6.22E+03	0.64028984	0	2.58155836	0	0
11/3/2018	e3_a5	1.54628393	1.34E+04	0.45594983	0	0	0	0
11/3/2018	e3_a5_rp	2.38129941	4.14E+03	0	0	0	0.96182919	0
11/3/2018	e3_a6	2.3040909	4.14E+03	0.70517723	0	0	0.96182919	0
11/3/2018	e3_a6_rp	2.11944862	8.04E+03	0	0	2.00430734	0	0
11/3/2018	e3_a7	2.22333971	7.10E+03	0.45594983	0	0	0	0.42120126
11/3/2018	e3_a7_rp	2.11944862	6.22E+03	0	0	1.73578758	0.96182919	0
11/3/2018	e3_a8	2.40353749	5.61E+03	0	0	0	0	0
11/3/2018	e3_a8_rp	2.38129941	1.93E+03	0.45594983	0	1.73578758	1.01448693	0
11/3/2018	e3_a9	2.06837671	1.04E+04	0	0	0	0	0
11/3/2018	e3_a9_rp	2.22333971	3.97E+03	0	0	0	1.01967332	0
11/3/2018	e3_a10	2.43429494	4.14E+03	0.69174071	0	0	0	0
11/3/2018	e3_a10_rp	2.2410179	5.03E+03	0	0	0	0.99610027	0
11/3/2018	e3_a11	1.69726049	1.31E+04	0	0	0	0	0
11/3/2018	e3_a11_rp	2.11944862	6.87E+03	0	0	0	0.97858492	0
11/3/2018	e3_a12	1.54628393	4.66E+03	0.70517723	0	0	0	0
11/3/2018	e3_a12_rp	2.38129941	4.14E+03	0	0	0	0.96182919	0
11/3/2018	e3_a13	2.0096936	3.13E+02	0.75106522	0.38338665	0	1.0339209	0
11/3/2018	e3_a13_rp	2.25786851	5.22E+03	0.69174071	0	0	0.93795033	0
11/3/2018	e3_a14	2.31823322	7.10E+03	0	0	0	0	0
11/3/2018	e3_a14_rp	2.27395886	6.22E+03	0	0	0	0.92172052	0
11/3/2018	e3_a15	2.34488423	5.22E+03	0	0	0	0.92172052	0
11/3/2018	e3_a15_rp	2.27395886	6.22E+03	0	0	0	0.92172052	0

11/3/2018	e3_a16	2.3040909	7.33E+03	0	0	0	0	0
11/3/2018	e3_a16_rp	2.27395886	6.22E+03	0	0	0	0.92172052	0
11/3/2018	e3_a17	2.38129941	4.84E+03	0	0	0	0	0.42316266
11/3/2018	e3_a17_rp	2.22333971	8.54E+03	0	0	0	0	0
11/24/2018	e3_a18	2.58607529	2.04E+03	0	0	0	0	0
11/24/2028	e3_a18_rp	1.44895111	2.04E+03	0.73203442	0	1.56418052	1.04488679	0
11/24/2028	e3_a19	1.3289623	5.61E+03	0.72760982	0	2.51883176	0	0.42640081
11/24/2028	e3_a19_rp	1.17458973	4.84E+03	0.69174071	0	2.88527146	0	0.4267887
11/24/2028	e3_a20	1.17458973	9.58E+03	0	0	2.74658066	0	0
11/24/2028	e3_a20_rp	1.17458973	1.07E+04	0	0	2.51883176	0	0
11/24/2028	e3_a21	0.96264175	1.22E+04	0	0	2.00430734	0	0.3949089
11/24/2028	e3_a21_rp	1.44895111	2.52E+03	0.64028984	0	2.1134536	1.04412491	0
11/24/2028	e3_a22	1.62766422	6.87E+03	0	0	3.00479699	0	0.34310436
11/24/2028	e3_a22_rp	0.96264175	8.29E+03	0.58320933	0	1.07739731	1.01151981	0
11/24/2028	e3_a23	1.75783013	1.10E+04	0	0	1.88001247	0	0
11/24/2028	e3_a23_rp	1.44895111	1.19E+04	0	0	2.00430734	0	0
11/24/2028	e3_a24	1.17458973	1.16E+04	0	0	2.29835828	0	0
11/24/2028	e3_a24_rp	1.44895111	1.19E+04	0	0	2.00430734	0	0
12/13/2018	e3_a25	2.18518488	9.05E+03	0	0	0	0	0
12/13/2018	e3_a25_rp	0.96264175	1.28E+04	0	0	0.68466155	0	0.42316266
12/13/2018	e3_a26	0.63725803	1.07E+04	0	0	0	0.96182919	0.42120126
12/13/2018	e3_a26_rp	0.38589458	9.98E+03	0.58320933	0	1.88001247	0.96182919	0
12/13/2018	e3_a27	0.63725803	1.43E+04	0	0	1.46450251	0	0
12/13/2018	e3_a27_rp	0.96264175	1.36E+04	0.53420573	0	0	0	0.41095643
12/13/2018	e3_a28	0.63725803	1.42E+04	0.19355952	0.37596413	0	0	0
12/13/2018	e3_a28_rp	0.63725803	1.22E+04	0	0	2.29835828	0	0
12/13/2018	e3_a29	1.17458973	1.44E+04	0	0.32061154	0	0	0
12/13/2018	e3_a29_rp	0.217128	1.24E+04	0.64028984	0.38116252	0	0	0.34310436
12/13/2018	e3_a30	0	1.09E+04	0.19355952	0	2.64009582	0	0
12/13/2018	e3_a30_rp	0	1.01E+04	0	0	1.3526283	0.99610027	0
12/13/2018	e3_a31	0.96264175	1.38E+04	0	0	1.56418052	0	0
12/13/2018	e3_a31_rp	0	1.01E+04	0	0	1.3526283	0.99610027	0
12/13/2018	e3_a32	0.96264175	1.13E+04	0	0	2.45128272	0	0
12/13/2018	e3_a32_rp	0	1.01E+04	0	0	1.3526283	0.99610027	0
12/13/2018	e3_a33	0.217128	1.55E+04	0	0	0.40255159	0	0
12/13/2018	e3_a33_rp	0	1.01E+04	0	0	1.3526283	0.99610027	0
12/29/2019	e3_a34	1.17458973	1.30E+04	0	0	1.77405815	0	0
12/29/2019	e3_a34_rp	1.44895111	1.01E+04	0	0	2.51883176	0	0
12/29/2019	e3_a35	0	8.29E+03	0	0	3.07617214	0	0
12/29/2019	e3_a35_rp	1.44895111	1.01E+04	0	0	2.51883176	0	0
12/29/2019	e3_a36	1.3289623	8.54E+03	0	0	2.1134536	0	0.42661959
12/29/2019	e3_a36_rp	0	1.01E+04	0	0	2.79531216	0	0
12/29/2019	e3_a37	0	1.58E+04	0	0	0	0	0
12/29/2019	e3_a37_rp	0.96264175	8.29E+03	0	0	2.92697661	0	0.3949089
12/29/2019	e3_a38	0	8.79E+03	0	0	3.00479699	0	0

12/29/2019	e3_a38_rp	1.54628393	7.80E+03	0	0	2.92697661	0	0
1/19/2019	e3_a39	1.44895111	4.31E+03	0	0	3.45683224	0	0
1/19/2019	e3_a39_rp	0	1.41E+04	0	0	1.73578758	0	0
1/19/2019	e3_a40	2.31823322	2.27E+03	0	0.3828252	2.79531216	0	0
1/19/2019	e3_a40_rp	0.217128	1.47E+04	0	0	1.3526283	0	0
1/19/2019	e3_a41	0.63725803	1.19E+04	0	0	1.88001247	0.87376449	0
1/19/2019	e3_a41_rp	0	4.90E+00	0.76331974	0	0	0.92172052	0
1/19/2019	e3_a42	0	0.00E+00	0.76277505	0	3.04122393	0	0
1/19/2019	e3_a42_rp	0	4.90E+00	0.76331974	0	0	0.92172052	0
1/26/2019	e3_a43	0	5.03E+03	0	0	3.47847532	0	0
1/26/2019	e3_a43_rp	0	1.25E+04	0	0	2.29835828	0	0
1/26/2019	e3_a44	1.54628393	5.41E+03	0	0.38308622	2.88527146	0	0
1/26/2019	e3_a44_rp	1.54628393	4.66E+03	0	0.38116252	1.88001247	1.00463565	0.4243748
1/26/2019	e3_a45	1.3289623	6.87E+03	0.69174071	0.37778966	0	0	0.42724486
1/26/2019	e3_a45_rp	1.17458973	6.01E+03	0	0.38231705	2.64009582	0.9510404	0
1/26/2019	e3_a46	0.63725803	9.05E+03	0	0.38308622	2.21070106	0	0
1/26/2019	e3_a46_rp	1.17458973	4.31E+03	0.58320933	0.38349333	1.3526283	0	0.42611163
1/26/2019	e3_a47	0.96264175	2.65E+03	0	0.38355158	1.07739731	0	0
1/26/2019	e3_a47_rp	0	1.71E+03	0.72203275	0.38317024	3.10975518	1.00060987	0
1/26/2019	e3_a48	1.17458973	1.38E+04	0	0	1.07739731	0	0.34310436
1/26/2019	e3_a48_rp	0	4.48E+03	0.58320933	0.38344313	0	1.01448693	0
1/26/2019	e3_a49	1.62766422	7.10E+03	0.58320933	0.38186868	2.58155836	0	0
1/26/2019	e3_a49_rp	0	4.48E+03	0.58320933	0.38344313	0	1.01448693	0
2/9/2019	e3_a50	0.63725803	6.43E+03	0	0.38351484	1.07739731	0	0
2/9/2019	e3_a50_rp	0.217128	1.25E+04	0	0.1691856	0.40255159	0.9510404	0
3/12/2019	e3_a51	0.8203389	1.16E+04	0.19355952	0	2.33913914	0	0.31211015
3/12/2019	e3_a51_rp	0.8203389	1.44E+04	0	0.1691856	0.68466155	0	0.3634649
3/12/2019	e3_a52	0.63725803	1.42E+04	0	0	0.99359488	0	0.3949089
3/12/2019	e3_a52_rp	0.38589458	6.27E+03	0	0	1.41027018	1.0339209	0
3/12/2019	e3_a53	1.3289623	1.19E+04	0.6498171	0.1691856	1.41027018	0	0.34310436
3/12/2019	e3_a53_rp	0.38589458	6.27E+03	0	0	1.41027018	1.0339209	0
3/12/2019	e3_a54	1.21737242	1.32E+04	0.45594983	0.1691856	1.29112817	0	0.26195757
3/12/2019	e3_a54_rp	0.38589458	6.27E+03	0	0	1.41027018	1.0339209	0
3/31/2019	e3_b1	0.63725803	1.26E+04	0.19355952	0	1.56418052	0	0.41882615
3/31/2019	e3_b1_rp	0.63725803	1.28E+04	0.64028984	0.32061154	1.07739731	0	0.3949089
3/31/2019	e3_a55	0.38589458	1.33E+04	0.64028984	0	1.07739731	0	0.3949089
3/31/2019	e3_a55_rp	0.96264175	1.13E+04	0.45594983	0.32061154	1.56418052	0.90104432	0
3/31/2019	e3_a56	0.96264175	1.01E+04	0.45594983	0.32061154	1.56418052	0.96182919	0
3/31/2019	e3_a56_rp	1.17458973	9.31E+03	0.45594983	0	1.07739731	0.99610027	0
3/31/2019	e3_a57	1.17458973	1.07E+04	0.45594983	0	2.00430734	0.87376449	0
3/31/2019	e3_a57_rp	1.17458973	9.31E+03	0.45594983	0	1.07739731	0.99610027	0
3/31/2019	e3_a58	0.96264175	1.44E+04	0	0.32061154	0.68466155	0	0
3/31/2019	e3_a58_rp	0.96264175	1.03E+04	0.31476588	0.32061154	1.07739731	0.78028918	0
4/27/2019	e3_a59	1.3289623	1.28E+04	0	0.37323225	1.07739731	0	0
4/27/2019	e3_a59_rp	1.75783013	8.54E+03	0	0	1.73578758	0.96182919	0
4/27/2019	e3_a60	2.06837671	9.05E+03	0	0.32061154	1.56418052	0	0
4/27/2019	e3_a60_rp	2.20475766	3.06E+03	0	0.36169067	2.1134536	1.01151981	0
Lambda Value =		-0.246064689	2.272906377	-1.306505823	-2.607123669	-0.035614709	-0.927119933	-2.338182845

VITA

Tegan Childers was born in Savannah, Georgia to parents, Jane and Dean Hendricks. While attending Dalton State College, she began working for their Turtle Assurance Colony. This is where her appreciation for herpetology and wildlife conservation began to grow. During her time at Dalton State, she engaged in amphibian research with her friend Daley Harrison. Her research advisors Chris Manis and John Lugthart encouraged her to continue in the field of wildlife research. She completed her Bachelors of Science degree in May of 2017 at Dalton State College. She then continued her turtle conservation work and passion for herpetology under the advisement of Thomas Wilson at the University of Tennessee at Chattanooga. Tegan graduated with a Master of Science degree in Environmental Science in August 2020. She anticipates continued work with conservation GIS, wildlife conservation and ecosystem management.